ELSEVIER

Catalytic asymmetric synthesis and anticancer effects of the novel non-calcemic analog of vitamin D, 2α-fluoro-19-nor-22-oxa-1α, 25-dihydroxyvitamin D₃ in metastatic lung carcinoma

Kimie Nakagawa [a], Toshio Okano [a,*], Keiichi Ozono [b], Shigeaki Kato [c], Noboru Kubodera [d], Shiho Ohba [e], Yoshimitsu Itoh [e], Koichi Mikami [e,*]

[a] *Department of Hygienic Sciences, Kobe Pharmaceutical University, Kobe 658-8558, Japan*
[b] *Department of Developmental Medicine, Pediatrics, Osaka University Graduate School of Medicine, Osaka 565-0871, Japan*
[c] *Institute of Molecular and Cellular Bioscience, University of Tokyo, Tokyo 113-0032, Japan*
[d] *Chugai Pharmaceutical Co. Ltd., Tokyo 104-8301, Japan*
[e] *Department of Applied Chemistry, Tokyo Institute of Technology, Tokyo 152-8552, Japan*

Abstract

1α,25-Dihydroxyvitamin D_3 (1α,25-D_3) has potent antiproliferative and anti-invasive properties *in vitro* in cancer cells. However, the major limitation to its clinical use is that it causes hypercalcemia. Therefore, vitamin D analogs with potent cell regulatory effects but with weaker calcemic effects than 1α,25-D_3 are required. Among them, 22-oxa-1α,25-D_3 and 19-nor-1α,25-D_3 have anti-cancer effects with relatively low calcemic effects. Modifications at the C-2α position of the A-ring also produced analogs with a unique biological profile. Not only the side-chain but also the A-ring modification thus generates a unique analog with potent cell regulatory effects and low calcemic activity as well. We report here that the hybrid 1α,25-D_3 analog, synthesized via the highly regio- and stereo-selective ring opening 2α-fluorination and catalytic asymmetric carbonyl-ene cyclization, with 2α-fluoro, 19-nor, and 22-oxa modification exhibits unique cell regulatory activities against the development of metastatic lung carcinoma.

© 2007 Published by Elsevier B.V.

Keywords: 2α-F-19-nor-22-oxa-1α,25-D_3; Non-calcemic; Lung cancer; Metastasis

1. Introduction

The physiologically active form of vitamin D_3, 1α,25-D_3 [1], plays a key role in the regulation of calcium homeostasis in mammals (Fig. 1). 1α,25-D_3 also exerts cell regulatory effects in target cells [2–4]. The exact mechanism of action of 1α,25-D_3 in target cells has not been clarified, but it is well accepted that 1α,25-D_3 first binds to the nuclear vitamin D receptor (VDR) [5], a member of the superfamily of steroid receptors [6,7]. The 1α,25-D_3-liganded VDR then heterodimerizes with the retinoid X receptor (RXR) [8] and subsequently this complex binds to the vitamin D-responsive elements (VDREs) in the promoter regions of the primary responding genes, leading to either activation or suppression of gene transcription [9]. The broad distribution of VDR in many tissues and the fact that 1α,25-D_3 modulates proliferation and differentiation of normal and malignant cells make this hormone a potentially useful agent for the treatment of diseases such as cancer [10], psoriasis [11,12], and immune disorders [13]. However, the major limitation to its clinical use is that it causes hypercalcemia [14]. Therefore, vitamin D analogs with potent cell regulatory effects but with weaker calcemic effects than 1α,25-D_3 are required [15].

The chemical synthesis of analogs is generally carried out for a variety of reasons; one is to increase potency, and another is to increase selectivity and further to diminish toxicity. The long history of the syntheses of analogs of 1α,25-D_3 has yielded a number of important compounds that have been clearly developed for therapeutic use; 1α,25-D_3 itself, 25-hydroxyvitamin D_3 (25-OH-D_3), 1α-hydroxyvitamin D_3 (1α-OH-D_3), 1α-hydroxyvitamin D_2 (1α-OH-D_2), 22-oxa-1α,25-D_3, 19-nor-1α,25-D_2,
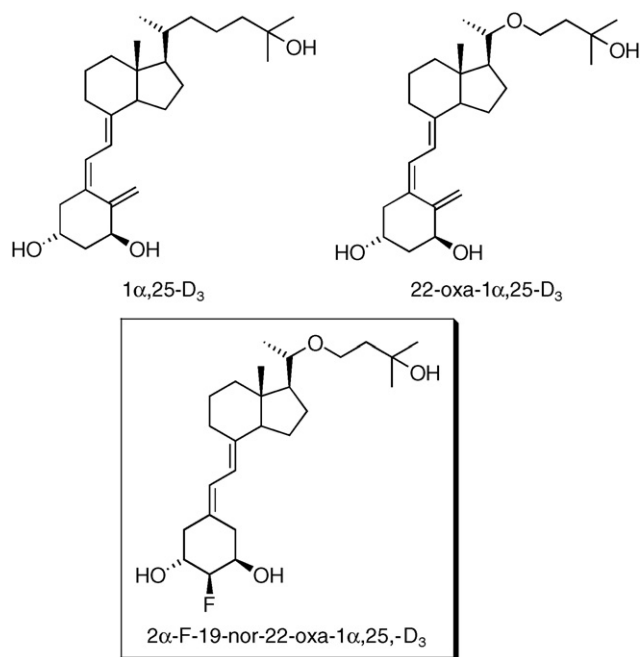
Fig. 1. Chemical structures of 22-oxa-1α,25-D₃ and 2α-substituted 19-nor-22-oxa-1α,25-D₃ analogs referred to in this report.

and calcipotriol [16–22]. The selectivity or reduced toxicity achieved in these cases is largely the result of rapid metabolic inactivation rather than selective activity of the analog at the molecular level. There remains, therefore, a great demand for analogs of 1α,25-D₃ that are selective in their activities, that are safe as much as they do not cause hypercalcemia, and that retain high potency.

explosively been investigated. 2-Fluoro-1α,25-dihydroxyvitamin D₃ (2-F-1α,25-D₃) was previously synthesized, however, only in the 2β form from steroidal 1,2α-epoxy 3β-ol because of the steric and electronic effects of 19-methyl group and A-ring (Eq. (1)) [30]; the corresponding 1,2β-epoxy 3β-ol gave the 1α-fluorinated regioisomer (Eq. (2)) not the 2α-F stereoisomer [31]. Therefore, the introduction of 2α-F group requires an acyclic epoxyalcohol precursor rather than the cyclic one for the highly regio- and stereo-selective ring opening 2α-fluorination (Fig. 2); We have thus developed a selective fluorinating reagent, group IV metal fluorides/ammonium hydrogen fluoride [32,33]. In the subsequent asymmetric carbonyl-ene cyclization catalyzed by (6-Br-)BINOL-Ti complexes [34,35], olefinic Z/E-geometrical control of A-ring can be translated, on the basis of the ''molecular symmetry'', into the α/β-configurational control of fluorine group at C-2, respectively.

During the course of our investigation of 2α-F-1α,25-D₃, we have focused on the 19-nor and 22-oxa derivatives because they appear to reduce the hypercalcemic activity of 1α,25-D₃ (Fig. 1): 2α-F-19-nor-22-oxa-1α,25-D₃ [38] as well as 19-nor-22-oxa-1α,25-D₃ [39]. First, we evaluated their biological properties in terms of binding affinity for VDR and serum vitamin D-binding protein (DBP), and transcriptional activity on the vitamin D target gene. 2α-F-19-nor-22-oxa-1α,25-D₃ had transcriptional activity on rat 25-hydroxyvitamin D₃-24-hydroxylase gene as equipotent as 1α,25-D₃ and two-fold as strong as 22-oxa-1α,25-D₃. 2α-F-19-nor-22-oxa-1α,25-D₃ is the most potent analog on VDR-dependent transcriptional activity [38].

We have further developed the animal model of anti-cancer effects of vitamin D analogs, a highly metastatic model using
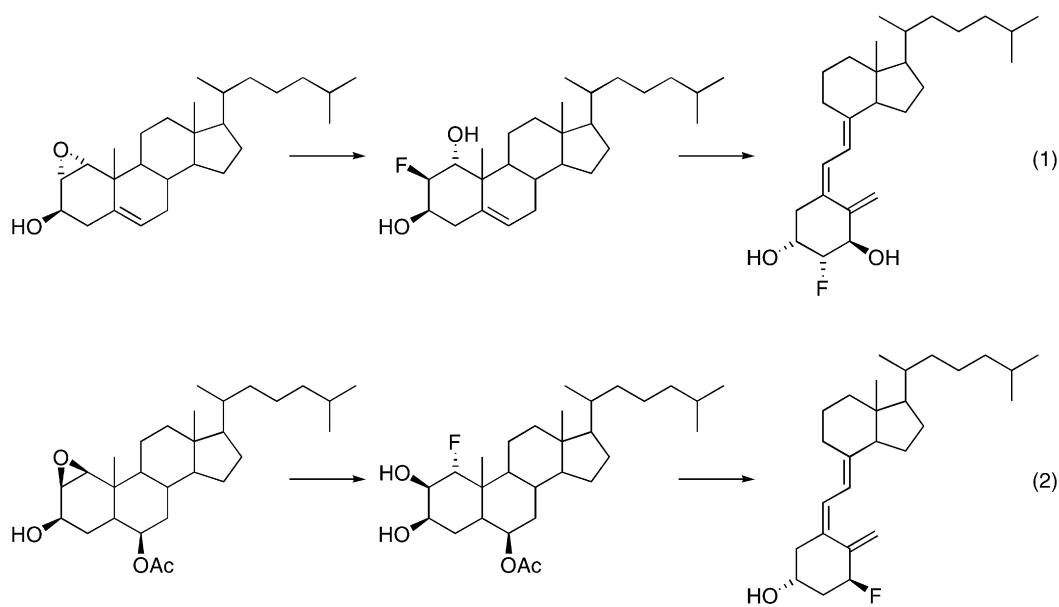
Organofluorine compounds have attracted much attention, because of their great importance as biologically active agents, which exhibit specific biological properties [23–29]. Therefore, the selective fluorination to modify biological activity has

Lewis lung carcinoma (LLC) cells expressing green fluorescent protein (GFP) [41]. LLC has been an important tumor model for studies of metastasis and angiogenesis and neoadjuvant chemotherapy. A major advantage of GFP-expressing LLC
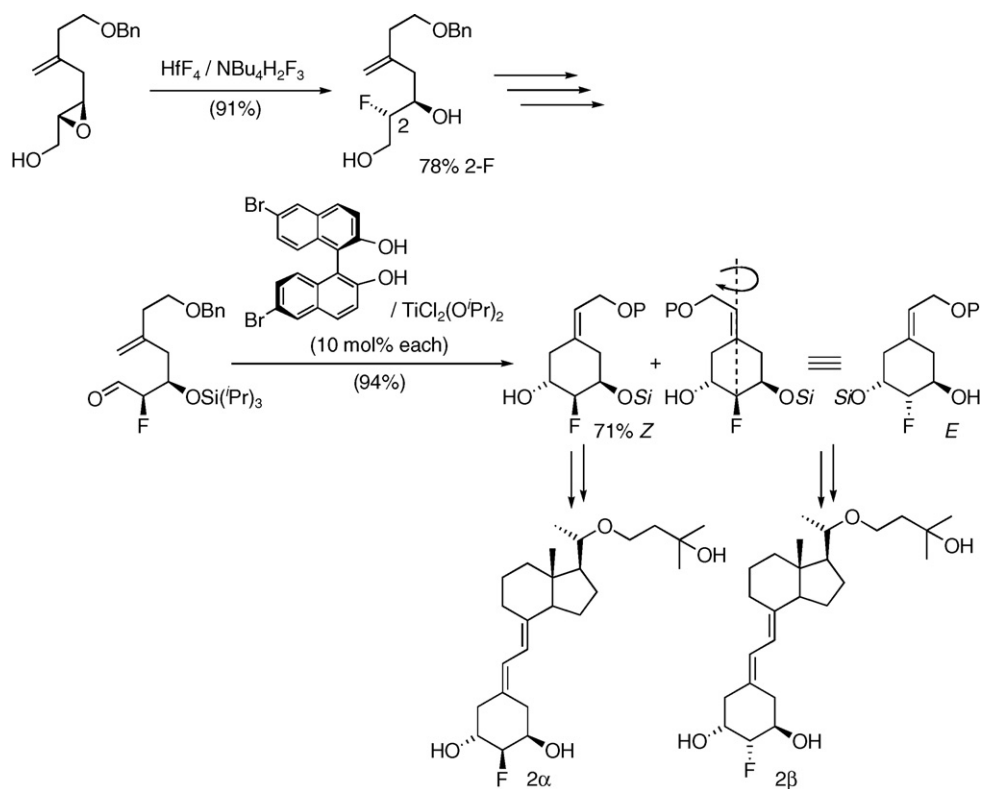
Fig. 2. Synthetic strategy for 2α-F-19-nor-22-oxa-1α,25-D$_3$ based on 2α-fluorination of acyclic epoxyalcohol and catalytic asymmetric carbonyl-ene cyclization.

(LLC-GFP) cells is that imaging requires no preparative procedures. The method is, therefore, suitable for visualizing live tissue during tumor progression. In addition, GFP labeling is extremely effective for measuring the number and volume of metastatic nodules in target organs. It has previously been reported that VDR knockout ($VDR^{-/-}$) mice with corrected hypocalcemia and hypervitaminosis D being fed a high calcium and vitamin D-deficient diet can be used as an experimental model for screening the anti-cancer effects of new vitamin D analogs in vivo [42]. Our studies using the experimental model of LLC-GFP cells injected wild-type ($VDR^{+/+}$) and $VDR^{-/-}$ mice, have shown that 22-oxa-1α,25-D$_3$ reduced the metastasis of lung cancer cells without increasing the serum calcium concentration [41]. The weaker calcemic effect is mainly attributed to its short half-life in the blood stream [40]. However, high dose administration induced hypercalcemia in $VDR^{+/+}$ mice.

The purpose of the present study was to examine the effectiveness and weak calcemic effect even in high dose of 2α-F-19-nor-22-oxa-1α,25-D$_3$ in the preclinical treatment of animal model of metastatic lung cancer using LLC-GFP cells.

2. Results and discussion

2.1. Catalytic asymmetric synthesis of 2α-fluoro-19-nor-22-oxa-1α,25-dihydroxyvitamin D$_3$ A-ring analog

2α-Fluorinated (2α-F) [38] A-ring analog was synthesized according to the scheme shown in Fig. 3. The key step for the

stereoselective introduction of fluorine atom was achieved via the highly regio- and stereo-selective ring opening 2α-fluorination of chiral epoxy alcohol mediated by Lewis acid metal fluoride/ammonium hydrogen fluoride ((iv) in Fig. 3) [32,33]. The use of Hf, which has large ionic radii, leads to 2-selective ring opening fluorination. Asymmetric induction of 3-OH group was accomplished by the asymmetric carbonyl-ene cyclization catalyzed by BINOL-Ti catalyst ((viii) in Fig. 3) [34,35]. The geometrical (Z/E) and enantioselectivities over the newly formed olefin and 3-OH group depend on the chirality matching of the 6,6′-dibromo-1,1′-bi-2-naphtol (6,6′-Br$_2$-BINOL) ligand and 1-OH group. Finally, 2α-F-19-nor-22-oxa-1α,25-D$_3$ was synthesized via Lythgoe coupling [36,37] and subsequent deprotection of the silyl group (Fig. 3).

2.2. Effect on anti-proliferative activity and differentiation-inducing activity in HL-60 cells

Their in vitro and in vivo biological activities were compared with those of 22-oxa-1α,25-D$_3$ which is known to be a less calcemic and more potent against VDR-mediated gene expression than a natural hormone 1α,25-D$_3$. 22-Oxa and 19-nor analogs of 1α,25-D$_3$ are known to hardly bind to serum DBP which functions as a carrier protein of vitamin D derivatives in blood circulation. In our previous report, it is shown that 2α-F-19-nor-22-oxa-1α,25-D$_3$ has extremely weak DBP binding potency [38]. In contrast, it has VDR binding potency approximately four times as strong as that of 19-nor-22-oxa-1α,25-D$_3$ and much higher than that of 22-oxa-1α,
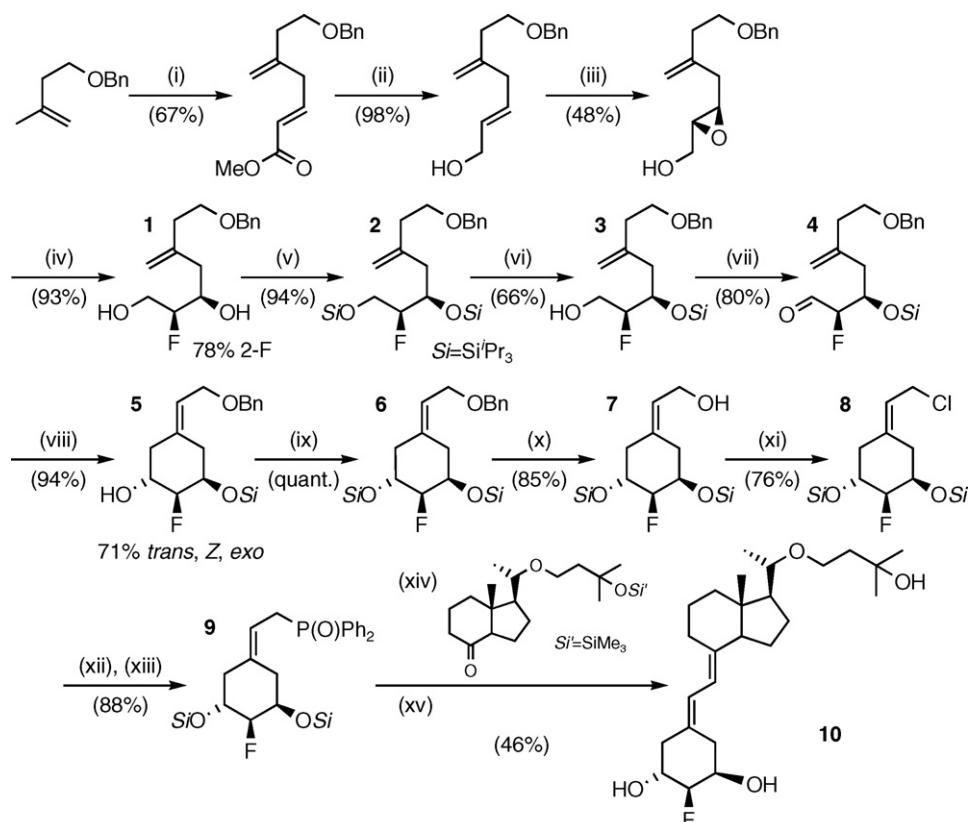
Fig. 3. Synthesis of 2α-F-19-nor-22-oxa-$1\alpha,25$-D_3. (i) $\equiv$–CO_2Me, $EtAlCl_2$, CH_2Cl_2, r.t.; (ii) DIBAL-H, CH_2Cl_2, $-78\,°C$; (iii) $Ti(O^iPr)_4$ (20 mol%), (−)-Diethyltartrate (DET) (24 mol%), TBHP, MS4A, CH_2Cl_2, $-30\,°C$; (iv) HfF_4, $Bu_4NH_2F_3$ (1.0 equiv. each), THF, r.t.; (v) triisopropylsilyltriflate (TIPSOTf), 2,6-lutidine, CH_2Cl_2, $0\,°C$; (vi) HF/Py, Et_3N, THF, r.t.; (vii) pyridinium chlorochromate (PCC), MS3A, CH_2Cl_2, r.t.; (viii) (R)-$6,6'$-Br_2-BINOL-Ti (10 mol%), CH_2Cl_2, r.t.; (ix) TIPSOTf, 2,6-lutidine, CH_2Cl_2, $0\,°C$; (x) Li, NH_3, ^tBuOH, Et_2O, $-78\,°C$ to r.t.; (xi) N-chlorosuccinimide (NCS), Me_2S, CH_2Cl_2, $-20\,°C$; (xii) Ph_2PLi, THF, $-78\,°C$ to r.t.; (xiii) H_2O_2, CH_2Cl_2, r.t.; (xiv) ^nBuLi, THF, $-78\,°C$ to r.t.; (xv) tetrabutylammonium fluoride (TBAF), THF, r.t.

25-D_3. Moreover, we reported that the 2α-F-19-nor-$1\alpha,25$-D_3 shows the significant activity in transactivation [38]. In the present study, we examined the anti-cancer effects of 2α-F-19-nor-22-oxa-$1\alpha,25$-D_3. Effects of 19-nor analogs on cell cycle phase distribution and cell-surface CD11b antigen expression in HL-60 cells was measured using FACS analysis. Table 1 indicates the relative activity of the analogs compared with 50% effective concentration (EC_{50}) of $1\alpha,25$-D_3. All the 19-nor-22-oxa analogs have weak effects on cell cycle G1 arrest and differentiation in HL-60 cells. Relative potency of 2α-F-19-nor-22-oxa-$1\alpha,25$-D_3 compared to 22-oxa-$1\alpha,25$-D_3 was 51% in the G1 arrest-inducing activity and 23% in differentiation-

inducing activity. Effects of 2α-F-19-nor-22-oxa-$1\alpha,25$-D_3 were less potent than $1\alpha,25$-D_3 and 22-oxa-$1\alpha,25$-D_3.

2.3. Transactivations on target genes

A summary of the transcriptional effectiveness EC_{50} of all the analogs evaluated is reported for the MG-63 cells in Table 1. The order of the transcriptional activities on a rat 25(OH)D_3-24-hydroxylase gene promoter containing two VDREs in transfected MG-63 cells for the 19-nor-22-oxa-$1\alpha,25$-D_3 analogs is 22-oxa-$1\alpha,25$-D_3 > 2α-F-19-nor-22-oxa-$1\alpha,25$-D_3 > $1\alpha,25$-D_3 > 19-nor-22-oxa-$1\alpha,25$-D_3. 2α-F-19-nor-22-oxa-$1\alpha,25$-D_3 exhibited

Table 1
Biological activities of 19-nor-22-oxa-$1\alpha,25(OH)_2D_3$ analogs

Compound	Rat serum DBP[*]	HL-60 cells[#]		Transcriptional potency (MG-63 cells)[#]			
		Diff. CD11b	Cell cycle G1 arrest	Rat 24OHase	VDR-GAL	RXRα-GAL	VDR/SRC-1
$1\alpha,25$-D_3	100	100	100	100	100	100	100
22-oxa-$1\alpha,25$-D_3	0.3	85	172	270	730	243	23
19-nor-22-oxa-$1\alpha,25$-D_3	N.R.	12	44	20	220	31	15
2α-Me-19-nor-22-oxa-$1\alpha,25$-D_3	N.R.	10	52	60	280	93	46
2α-F-19-nor-22-oxa-$1\alpha,25$-D_3	N.R.	23	51	180	690	43	209

N.R.: not reached to 50% displacement of $[^3H]$-25(OH)D_3 or $[^3H]$-$1\alpha,25$-D_3; Not; not tested.
[*] Ref. [25].
[#] All results are expressed as percentage activity (at 50% of the dose response) in comparison with $1\alpha,25$-D_3 (=100% activity).

potency nearly as equipotent as 22-oxa-1α,25-D$_3$ and two-fold as strong as 1α,25-D$_3$. To determine whether transcriptional potency is associated with binding potency to VDR, we cotransfected an one-hybrid plasmid inserted with a human VDR cDNA connected with GAL-DBD and a luciferase reporter plasmid containing GAL-BS into MG-63 cells and treated the cells with various concentrations of 1α,25-D$_3$ and the analogs. We found that 2α-F-19-nor-22-oxa-1α,25-D$_3$ had potent *in situ* VDR-binding activity as equipotent as 22-oxa-1α,25-D$_3$ and seven-fold as strong as 1α,25-D$_3$. Moreover, we contrasted the ability of 1α,25-D$_3$, 22-oxa-1α,25-D$_3$ and 19-nor-22-oxa-1α,25-D$_3$ analogs to promote VDR interaction with RXRα and the p160 coactivators SRC-1 in the mammalian hybrid luciferase assay in MG-63 cells. All the 19-nor-22-oxa-1α,25-D$_3$ analogs had less potent as 22-oxa-1α,25-D$_3$ on VDR/RXR heterodimer-dependent transcriptional activity on RXR-GAL4 system. However, in VDR/SRC-1-GAL4 system, 2α-F-19-nor-22-oxa-1α,25-D$_3$ manifested a 10-fold and two-fold increase in potency over 22-oxa-1α,25-D$_3$ and 1α,25-D$_3$, respectively. On the other hand, 2α-F-19-nor-22-oxa-1α,25-D$_3$ is equally equipotent to 22-oxa-1α,25-D$_3$ and 1α,25-D$_3$. These results clearly indicate that 2α-F is a structural motif to enhance VDR binding and VDR/SRC-1 interaction potency and increase biological activity at the transcriptional level.

2α-F-19-nor-22-oxa-1α,25-D$_3$ displays low affinity for serum DBP as compared with 1α,25-D$_3$. These characteristics are likely to influence its pharmacokinetic properties and thus its actions *in vivo*. In this report, we focused upon the molecular mechanisms that underlie the enhanced potency of 2α-F-19-nor-22-oxa-1α,25-D$_3$. This potency is manifested in cell culture at the level of endogenous gene expression as well as transcription, despite the fact that both 2α-F-19-nor-22-oxa-1α,25-D$_3$ and 1α,25-D$_3$ bind equally well to VDR. Indeed, this property is a characteristic of many chemically related classes of vitamin D analogs, as herein shown using VDR-GAL4 and VDR/SRC-1 hybrid luciferase assays. Among three 19-nor-22-oxa-1α,25-D$_3$ analogs we tested, the strongest effects on VDR/SRC-1 interaction was only limited to 2α-F-19-nor-22-oxa-1α,25-D$_3$. Although 22-oxa-1α,25-D$_3$ has potent antiproliferative effects, it shows even weaker effect on SRC-1 binding to VDR than 1α,25-D$_3$. It has been reported that 22-oxa-1α,25-D$_3$ selectively induces VDR to interact with TIF2 but not with SRC-1 or AIB1/ACTR [42]. These results suggest that high potency of 2α-F-19-nor-22-oxa-1α,25-D$_3$ may be due to the ability of 2α-F modification to induce unique VDR conformations that favor enhanced interaction with coactivator such as SRC-1. These findings provide a molecular explanation for the increased potency of 2α-F-19-nor-22-oxa-1α,25-D$_3$ and together with previous studies may explain the potency of other vitamin D analogs that exhibit similar properties. Previously it has been reported that 2-methylene-19-nor-(20S)-1,25-dihydroxyvitamin D$_3$ (2MD) is a highly potent analog of 1α,25-D$_3$ whose actions are mediated through the VDR. 2MD is more potent in promoting interaction with RXR and the coactivators SRC-1 and DRIP205 [43]. Therefore, differences in VDR structure in the presence of 2α-F-19-nor-22-oxa-1α,25-D$_3$ may be responsible for the enhanced
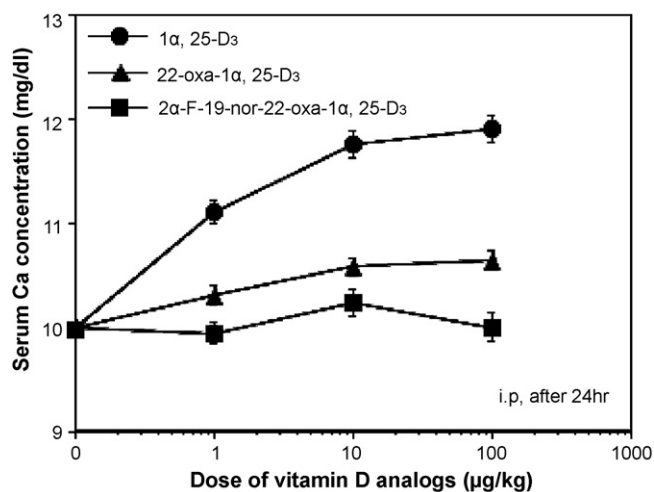
interactions of VDR with SRC-1 as well as 2MD, which is 19-nor and 2-substituted analog. The existence of multiple VDR coactivators may allow target cells to respond to different stimuli in a more specific manner. By comparing analog 2α-F-19-nor-22-oxa-1α,25-D$_3$ with 22-oxa-1α,25-D$_3$, or 19-nor-22-oxa-1α,25-D$_3$, we found a more profound effect on stabilization of the ligand within the receptor as a result of 2α-F introduction. Fluorine, being the most electronegative ion, may increase the overall negative charge on the surface of the receptor, though inside the ligand binding domain, acting as a recruitment enhancer for coactivators. While our findings focus primarily on the potency of 2α-F-19-nor-22-oxa-1α,25-D$_3$, they may well provide avenues to discover new vitamin D leads that possess highly potent and cell-specific anti-cancer effects.

2.4. Effect of 2α-F-19-nor-22-oxa-1α,25-D$_3$ on serum calcium

The *in vivo* calcemic effects of 2α-F-19-nor-22-oxa-1α,25-D$_3$ were assessed by monitoring serum calcium levels after oral injection. The dose–response effect of each analog was calculated at the time when the effect was maximum (after 24 h) and expressed as the dosage required to elevate the serum calcium level by 1 mg/dL (Fig. 4). 22-oxa-1α,25-D$_3$ causes mild hypercalcemia with insignificant decrease in body weight (data not shown). In contrast, the serum calcium remained nearly normal over a period of 72 h after oral injection in 2α-F-19-nor-22-oxa-1α,25-D$_3$ 100 μg/kg administration group. The results are in agreement with other *in vivo* studies using a maximum dose of 1 μg/kg body weight of 22-oxa-1α,25-D$_3$ [41]. Therefore, high concentration of 22-oxa-1α,25-D$_3$ could not be used for *in vivo* studies as it may cause calcemic side effects at >10 μg/kg. However, we found that higher doses (10 and 100 μg/kg) of 2α-F-19-nor-22-oxa-1α,25-D$_3$ singly injected did not cause hypercalcemia suggesting that high doses of 2α-F-19-nor-22-oxa-1α,25-D$_3$ may not cause adverse side effects. Initial characterization of these analogs reveals a significantly stronger activity than that of 1α,25-D$_3$; in particular, 2α-F-19-nor-22-oxa-1α,25-D$_3$ display a transactivation potency even or over that of 22-oxa-1α,25-D$_3$ and 19-nor-22-oxa-1α,25-D$_3$ while having a significantly lower calcemic index than 22-oxa-1α,25-D$_3$. Thus, 2α-F-19-nor-22-oxa-1α,25-D$_3$ is excellent target for further analysis and development of the therapeutic agent of cancers.

2.5. Effects of 1α,25-D$_3$ and 2α-F-19-nor-22-oxa-1α,25-D$_3$ on cell growth and metastatic activity of LLC-GFP cells in vitro

We examined the effects of 1α,25-D$_3$, 22-oxa-1α,25-D$_3$ and 2α-F-19-nor-22-oxa-1α,25-D$_3$ on the proliferation and invading activity of lung cancer LLC-GFP cells *in vitro*. As shown in Fig. 5a, treatment with 10^{-7} M of 1α,25-D$_3$, 22-oxa-1α,25-D$_3$, 19-nor-22-oxa-1α,25-D$_3$ and 2α-F-19-nor-22-oxa-1α,25-D$_3$ for 3 days resulted a significant arrest of the cell cycle at G0/G1 in LLC-GFP cells. The order of potency of the cell cycle arrest inducing activities for these analogs in LLC-GFP cells is

Fig. 4. Effects of 2α-F-19-nor-22-oxa-1α,25-D$_3$ on serum calcium. Mice were divided into several groups of six mice, each receiving oral administration of 1, 10 or 100 μg/kg of 1α,25-D$_3$ or its analogs in 2 μL/kg of 0.1% Triton X-100 solution. The resulting increases in serum calcium were measured at 24 h after administration by the *o*-cresolphthalein complexone (OCPC) method. The relative activity of each analog with respect to 1α,25-D$_3$ was evaluated as follows: the dose–response effect of each analogue was calculated at the time when the effect was maximum and expressed as the dosage required to elevate the serum calcium level by 1 mg/dL.

Fig. 5. Effects of 2α-F-19-nor-22-oxa-1α,25-D$_3$ on LLC-GFP cell growth and metastasis *in vitro*. (a) Cell cycle phase distribution in 1α,25-D$_3$, 22-oxa-1α,25-D$_3$, 19-nor-22-oxa-1α,25-D$_3$ or 2α-F-19-nor-22-oxa-1α,25-D$_3$ treated-LLC-GFP cells at 72 h. (b) The capacity of 1α,25-D$_3$, 22-oxa-1α,25-D$_3$, 19-nor-22-oxa-1α,25-D$_3$ or 2α-F-19-nor-22-oxa-1α,25-D$_3$ treated-LLC-GFP cells to transverse a Matrigel-coated filter for 24 h. Each bar represents the mean ± S.E. **,##: $P < 0.01$ and ***,###: $P < 0.001$ ($n = 6$).

22-oxa-1α,25-D$_3$ > 2α-F-19-nor-22-oxa-1α,25-D$_3$ = 1α,25-D$_3$ > 19-nor-22-oxa-1α,25-D$_3$.

A prior study showing reduced random migration by LLC-GFP cells after 3 days of incubation with 1α,25-D$_3$ determined the effect of increasing concentrations of 1α,25-D$_3$ on tumor cell invasiveness through reconstituted basement membrane-coated filters [44]. The vehicle-treated LLC-GFP cells readily transversed the matrix-coated membranes. In contrast, incubation with 1α,25-D$_3$ and these analogs caused a dose-dependent decline in the invasive capability of the tumor cells. The order of potency of the anti-metastatic activities for these analogs in LLC-GFP cells is 22-oxa-1α,25-D$_3$ > 2α-F-19-nor-22-oxa-1α,25-D$_3$ = 1α,25-D$_3$ > 19-nor-22-oxa-1α,25-D$_3$. 2α-F-19-nor-22-oxa-1α,25-D$_3$ had potent anti-invading activity in LLC-GFP cells nearly as equipotent as 22-oxa-1α,25-D$_3$ and significantly as strong as 19-nor-22-oxa-1α,25-D$_3$ (Fig. 5b). The modifications upon the A-ring with 2α-F increased the anti-metastatic activity in LLC-GFP cells compared with 19-nor-22-oxa-1α,25-D$_3$. We therefore believe that the structural modification reported for 2α-F-19-nor-22-oxa analogs could serve as basis for the development of therapeutic agents for the metastatic cancers that can mimic the low calcemic effects while retaining the strong anti-metastatic capability.
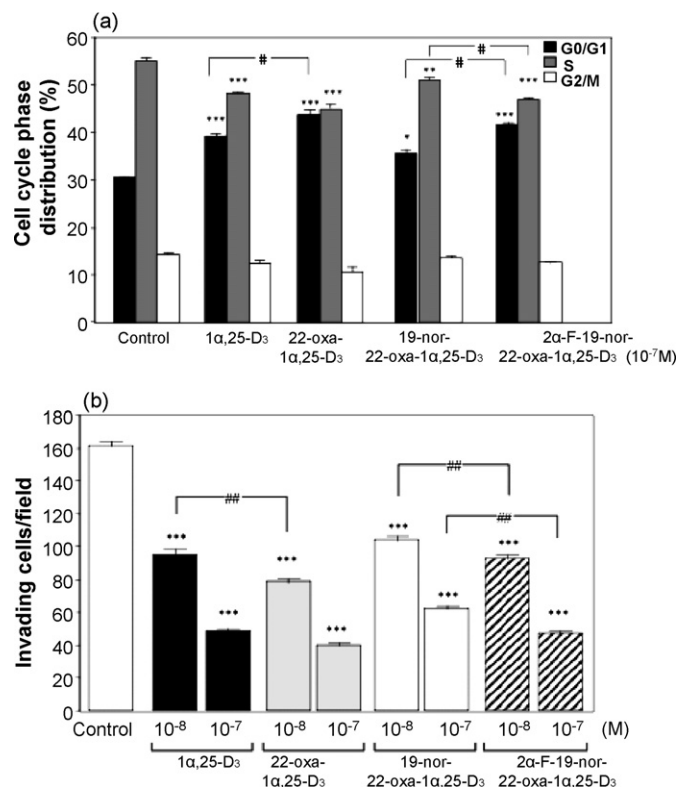
2.6. Effects of continuous treatment with 2α-F-19-nor-22-oxa-1α,25-D$_3$ on the development of lung metastases in the LLC-GFP cell injected VDR$^{+/+}$ mice and VDR$^{-/-}$ mice fed a high calcium and vitamin D-deficient diet

The number of mice that developed lung metastases was analyzed by measuring the lung weight, nodule count and GFP mRNA expression in the lung by quantitative RT-PCR. VDR$^{-/-}$ mice exhibit hypocalcemia and extremely high serum levels of 1α,25-D$_3$ [45]. However, we previously reported that feeding these animals a high calcium and vitamin D-deficient diet resulted in the complete elimination of 1α,25-D$_3$ and correction of calcium in the serum of both VDR$^{+/+}$ and VDR$^{-/-}$ mice [44]. Our recent report suggests that VDR$^{-/-}$ mice with corrected hypocalcemia and hypervitaminosis D can be used as an experimental model for screening the anti-cancer effects of new vitamin D analogs *in vivo* [41,44]. In this study using this experimental model, 2α-F-19-nor-22-oxa-1α,25-D$_3$ was administered by an osmotic minipump for 3 weeks. LLC-GFP cells were injected into VDR$^{+/+}$ mice receiving a high dose of 2α-F-19-nor-22-oxa-1α,25-D$_3$ (50 μg/kg/day) and these animals subsequently showed insignificant hypercalcemia. VDR$^{-/-}$ mice receiving a high dose of 2α-F-19-nor-22-oxa-1α,25-D$_3$ and similarly injected with tumor cells did not show any
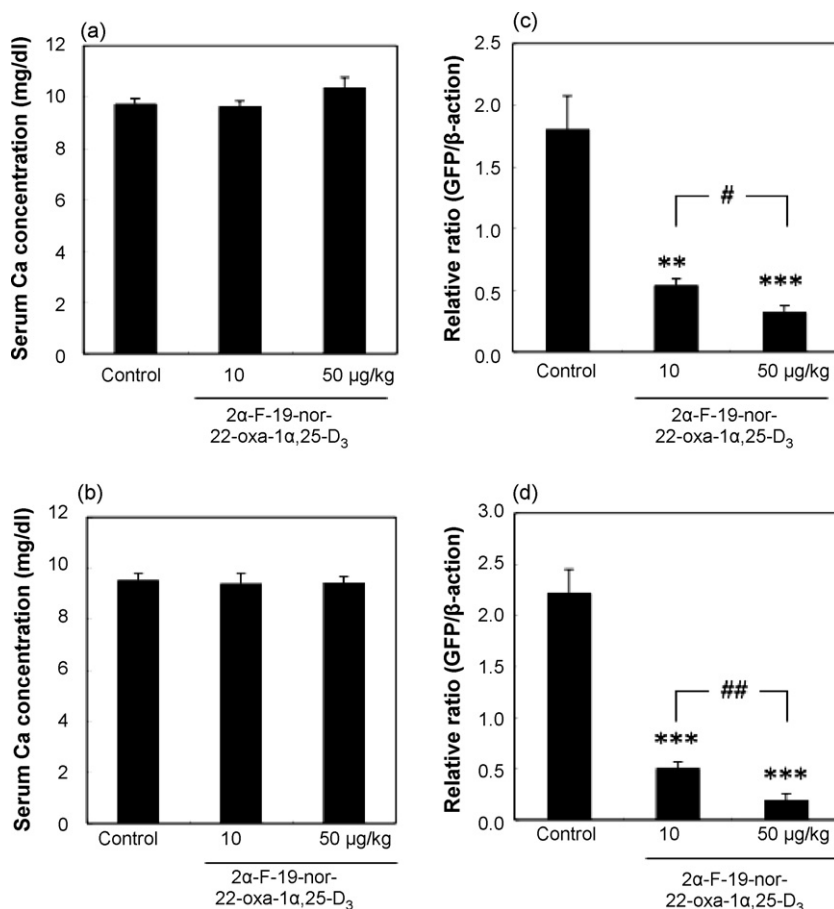
Fig. 6. Effects of continuous treatment with 2α-F-19-nor-22-oxa-1α,25-D_3 on the development of lung metastases in LLC-GFP cell-injected $VDR^{+/+}$ mice and $VDR^{-/-}$ mice fed a high calcium and vitamin D-deficient diet. 2α-F-19-nor-22-oxa-1α,25-D_3 (10 or 50 μg/kg/day) or vehicle was infused continuously by an osmotic minipump implanted s.c. on the same day as the LLC-GFP cell injection. Serum and lungs were collected on 3 weeks after the cell injection. (a and c) Serum calcium concentration and GFP mRNA expression of the lung in LLC-GFP cell injected $VDR^{+/+}$ mice. (b and d) Serum calcium concentration and GFP mRNA expression of the lung in LLC-GFP cell injected $VDR^{-/-}$ mice. Each bar represents the mean ± S.E. ($n = 10$). ***: $P < 0.001$ significant difference from vehicle treated animals. ##: $P < 0.01$ and ###: $P < 0.001$ significant difference from 2α-F-19-nor-22-oxa-1α,25-D_3 (10 μg/kg/day) treated animals.

significant change in serum calcium levels when compared with the vehicle-treated control group (Fig. 6a and b).

The number of mice that developed lung metastases was analyzed by measuring the GFP mRNA expression in the lung by quantitative RT-PCR. This parameter was significantly lower in the 2α-F-19-nor-22-oxa-1α,25-D_3-treated group than in the untreated group among $VDR^{+/+}$ mice and $VDR^{-/-}$ mice fed a high calcium and vitamin D-deficient diet (Fig. 6c and d). The anti-tumor effect of 2α-F-19-nor-22-oxa-1α,25-D_3 in $VDR^{+/+}$ mice and $VDR^{-/-}$ mice were dosed dependently. This result indicates that 2α-F-19-nor-22-oxa-1α,25-D_3 can act directly on cancer cells under conditions without calcemic activity and other actions of 2α-F-19-nor-22-oxa-1α,25-D_3 in the host. These results indicate that 2α-F-19-nor-22-oxa-1α,25-D_3 is less calcemic and more effective than 22-oxa-1α,25-D_3 in suppressing metastatic tumor growth of LLC-GFP cells. Its anti-tumor efficacy combined with non-calcemic effects (at 10 higher dose than 22-oxa-1α,25-D_3) suggest that higher concentrations of 2α-F-19-nor-22-oxa-1α,25-D_3 could be used.

Because dose-limiting hypercalcemia of the vitamin D analogs limits the therapeutic potential, identification of low-calcemic analogs is critical in vitamin D_3-mediated anticancer therapies. Among the recently discovered vitamin D_3 analogs, EB1089 (1α,25-dihydroxy-22,24-diene-24,26,27-trihomovitamin D_3), QW-1624F2-2 (1-hydroxymethyl-16-ene-24,24-F2-26,27-bishomo-25-hydroxyvitamin D_3) and 22-oxa-1α,25-D_3 might find clinical use [46]. More recently, we studied the effectiveness of 22-oxa-1α,25-D_3 on metastatic lung cancer. Low dose (1 μg/kg/day) of 22-oxa-1α,25-D_3 showed effectiveness similar to that of 1α,25-D_3 in continuous treatment of metastatic lung tumors in $VDR^{+/+}$ and $VDR^{-/-}$ mice without hypercalcemia. However, high dose (10 μg/kg/day) administration of 22-oxa-1α,25-D_3 caused hypercalcemia in $VDR^{+/+}$ mice [41]. The conclusion regarding the reduced-calcemic, synthetic vitamin D analogs including 22-oxa-1α,25-D_3 is that while their effectiveness appears sufficiently promising for clinical trials, their hypercalcemia-related toxicity remains problematic.

Therefore, we invented A-ring and side-chain hybrid vitamin D analogs that retain the potent transcriptional activity on vitamin D target genes and anti-cancer effects but are much less likely to raise serum calcium *in vivo*. 2α-F-19-nor-22-oxa-1α,25-D_3 is a new non-calcemic vitamin D analog in A-ring and side-chain modified analogs. In the present study, we

demonstrated that 2α-F-19-nor-22-oxa-1α,25-D$_3$ reduces the development of lung metastases without calcemic activity. The mechanisms by which 2α-F-19-nor-22-oxa-1α,25-D$_3$ inhibits tumor growth are not fully understood. In this study, 2α-F-19-nor-22-oxa-1α,25-D$_3$ induced growth arrest at G0/G1 in LLC-GFP cells. Moreover, 2α-F-19-nor-22-oxa-1α,25-D$_3$ significantly inhibited tumor invasive activity. We previously indicated that 1α,25-D$_3$ and 22-oxa-1α,25-D$_3$-treated LLC-GFP cells decreased metastatic activity and mRNA expression of MMP-2 and MMP-9, a family of proteases capable of degrading extracellular matrix and basement membrane components including collagens under physiological conditions [41]. Therefore, 2α-F-19-nor-22-oxa-1α,25-D$_3$ may mediate the expression of MMP-2 and MMP-9 genes in LLC-GFP cells. Obviously, the mechanisms underlying the anti-cancer effects of 2α-F-19-nor-22-oxa-1α,25-D$_3$ are complex and further investigation within this area is required in order to obtain a better understanding.

In vivo experiments that monitor serum calcium suggest that 2α-F-19-nor-22-oxa-1α,25-D$_3$ less calcemic than 22-oxa-1α,25-D$_3$. In continuous administration of 2α-F-19-nor-22-oxa-1α,25-D$_3$ using minipump, 2α-F-19-nor-22-oxa-1α,25-D$_3$ did not induce any adverse effects. The body weight of the mice remained normal and serum calcium levels did not cause any side effects. The *in vivo* efficacy data suggest that 2α-F-19-nor-22-oxa-1α,25-D$_3$ is more effective than 22-oxa-1α,25-D$_3$ in suppressing metastatic lung tumors. Its antitumor efficacy combined with non-calcemic effects suggested that higher concentrations of 2α-F-19-nor-22-oxa-1α,25-D$_3$ could be used for cancer therapy. The differences in the effectiveness between 2α-F-19-nor-22-oxa-1α,25-D$_3$ and 22-oxa-1α,25-D$_3$ could be due to differential catabolism or differential liganded-VDR interaction with coactivators. It is possible that 2α-F-19-nor-22-oxa-1α,25-D$_3$ might be hard to be metabolized and strongly promote the interaction of the VDR with potential facilitators of transactivation such as SRC-1 in cells.

Our recent report suggests that $VDR^{-/-}$ mice with corrected hypocalcemia and hypervitaminosis D can be used as an experimental model to screen the anti-cancer effects of new vitamin D analogs *in vivo* [44]. In this study using this experimental model, 2α-F-19-nor-22-oxa-1α,25-D$_3$ was administered for 3 weeks using an osmotic minipump. The LLC-GFP cells injected $VDR^{-/-}$ mice receiving a high dose of 2α-F-19-nor-22-oxa-1α,25-D$_3$ (50 μg/kg/day) did not show hypercalcemia and significantly decreased the tumor growth. This result clearly indicates that 2α-F-19-nor-22-oxa-1α,25-D$_3$ can act directly on cancer cells under conditions without calcemic activity or other actions of 2α-F-19-nor-22-oxa-1α,25-D$_3$ in the host. The high dose of 2α-F-19-nor-22-oxa-1α,25-D$_3$ does not cause hypercalcemia and loss of body weight in $VDR^{+/+}$ mice. In the previous reports, it has been suggested that mice treated with 1α,25-D$_3$ experienced a severe loss of thymocytes, and that thymic atrophy resulted as a consequence of 1α,25-D$_3$-induced hypercalcemia [47,48]. Therefore, 2α-F-19-nor-22-oxa-1α,25-D$_3$ is highly effective in inhibiting the metastatic tumor growth without hypercalcemia. In this experiment, our findings of marked anti-metastatic effects of 2α-F-19-nor-22-

oxa-1α,25-D$_3$, achieved with significantly less toxicity in terms of hypercalcemia and weight loss than 1α,25-D$_3$ and 22-oxa-1α,25-D$_3$, suggest that 2α-F-19-nor-22-oxa-1α,25-D$_3$ may offer a therapeutic option in advanced lung carcinoma.

3. Conclusion

We have demonstrated that the hybrid analog with 2α-fluoro, 19-nor, and 22-oxa modification of 1α,25-D$_3$ exhibits unique cell regulatory activities and clearly identified the structural motifs responsible for non-calcemic and anti-metastatic activity. We synthesized the 2α-F-19-nor-22-oxa-1α,25-D$_3$ analog via the highly regio- and stereo-selective epoxide opening 2α-fluorination and catalytic asymmetric carbonyl-ene cyclization, and examined the effect of the 2α-F-analog as a prophylactic for the treatment of lung metastasis. The 2α-F-analog did not cause hypercalcemia or a significant increase in mortality. Toxicity from hypercalcemia has been the major deterrent in the use of vitamin D analogs in clinical trial. Lung cancer patients have a very poor prognosis. It is therefore important to develop a therapeutic agent with anti-proliferative and anti-metastatic effects, but which has minimal side-effects. The 2α-F-analog has potential usefulness in the treatment of these tumors and should be incorporated in clinical trials. These findings will provide useful information not only for the development of therapeutic agents for treatment of lung cancer and other metastatic cancers but also for studies on the structure-function relationship of 1α,25-D$_3$.

4. Experimental

4.1. Catalytic asymmetric synthesis of 2α-fluoro-19-nor-22-oxa-1α,25-dihydroxyvitamin D$_3$ A-ring analog

4.1.1. (2S, 3R)-5-[2-(Benzyloxy)ethyl]-2-fluoro-5-hexene-1,3-diol (1)

Ten millilitres test tube with argon inlet was charged with hafnium (IV) tetrafluoride (0.130 g, 0.51 mmol) and THF (2.0 mL) at 0 °C. To the suspension was added tetrabutylammonium dihydrogentrifluoride (H$_2$F$_3$NBu$_4$) (0.166 g, 0.55 mmol) in THF (0.5 mL) and stirred for 10 min at that temperature. (2R,3R)-5-[2-(Benzyloxy)ethyl]-2,3-epoxy-5-en-1-hexanol (96% ee) (0.130 g, 0.53 mmol) was added dropwise and stirred for 10 min and then the reaction mixture was warmed up to room temperature. After stirring for 24 h at that temperature, the reaction mixture was quenched with sat. sodium hydrogencarbonate. After usual workup, the residue was purified by silica-gel chromatography to give (2S,3R)-5-[2-(benzyloxy)ethyl]-2-fluoro-5-hexene-1,3-diol (1) and (2R,3S)-5-[2-(benzyloxy)ethyl]-3-fluoro-5-hexene-1,2-diol (0.132 g, 94%) as the regioisomer in a ratio of 78:22.

4.1.1.1. (2S, 3R)-5-[2-(Benzyloxy)ethyl]-2-fluoro-5-hexene-1,3-diol (1). ^{19}F NMR (376 MHz, CDCl$_3$) δ −197.1 (dtd, $J = 47.0, 24.8, 9.0$ Hz, 1F); ^{1}H NMR (400 MHz, CDCl$_3$) δ 2.19 (dd, $J = 14.4, 2.0$ Hz, 1H), 2.39 (t, $J = 6.4$ Hz, 2H), 2.48 (d,

$J = 14.4$ Hz, 1H), 2.80 (bs, 1H), 3.25 (bs, 1H), 3.63 (t, $J = 6.4$ Hz, 2H), 3.85 (dd, $J = 24.8, 4.0$ Hz, 2H), 3.93–4.00 (m, 1H), 4.24–4.40 (ddt, $J = 47.2, 6.8, 4.0$ Hz, 1H), 4.51 (s, 2H), 4.98 (bs, 1H), 4.99 (bs, 1H), 7.29–7.35 (m, 5H); ^{13}C NMR (101 MHz, CDCl$_3$) δ 35.6, 40.6 (d, $^3J = 3.1$ Hz), 62.2 (d, $^2J = 21.4$ Hz), 68.6 (d, $^2J = 25.4$ Hz), 69.2, 73.2, 94.8 (d, $^1J = 173.8$ Hz), 114.9, 127.8, 127.9, 128.4, 137.8, 142.8.

4.1.1.2. (2R,3S)-5-[2-(Benzyloxy)ethyl]-3-fluoro-5-hexene-1,2-diol.

^{19}F NMR (376 MHz, CDCl$_3$) δ −190.4 (dddd, $J = 56.0, 46.6, 20.7, 10.2$ Hz, 1F); ^{1}H NMR (400 MHz, CDCl$_3$) δ 2.36–2.54 (m, 4H), 2.96 (bs, 1H), 3.08 (bs, 1H), 3.59 (t, $J = 6.8$ Hz, 2H), 3.65–3.73 (br, 3H), 4.51 (s, 2H), 4.50–4.68 (dddd, $J = 56.0, 9.2, 6.0, 3.2$ Hz, 1H), 4.94 (s, 1H), 4.96 (s, 1H), 7.29–7.35 (m, 5H); ^{13}C NMR (101 MHz, CDCl$_3$) δ 36.2, 38.0 (d, $^2J = 20.7$ Hz), 62.6 (d, $^3J = 5.4$ Hz), 68.8, 72.7 (d, $^2J = 23.7$ Hz), 73.0, 92.0 (d, $^1J = 173.1$ Hz), 114.1, 127.7, 127.9, 128.5, 138.2, 142.1.

4.1.2. (4R,5S)-2-[2-(Benzyloxy)ethyl]-5-fluoro-4,6-bis(triisopropylsilyloxy)-1-hexene (2)

To a solution of (2S,3R)-5-[2-(benzyloxy)ethyl]-2-fluoro-5-hexene-1,3-diol (**1**) and (2R,3S)-5-[2-(benzyloxy)ethyl]-3-fluoro-5-hexene-1,2-diol (2.53 g, 9.43 mmol) in CH$_2$Cl$_2$ (19 mL) was added 2,6-lutidine (2.86 mL, 24.5 mmol) and triisopropylsilyltriflate (TIPSOTf) (6.59 mL, 24.5 mmol) at 0 °C. After stirring for 1.5 h at that temperature, the reaction mixture was quenched with sat. sodium hydrogencarbonate. After usual workup, the residue was purified by silica-gel chromatography to give (4R,5S)-2-[2-(benzyloxy)ethyl]-5-fluoro-4,6-bis(triisopropylsilyloxy)-1-hexene (**2**) and (4S,5R)-2-[2-(benzyloxy)ethyl]-4-fluoro-5,6-bis(triisopropylsilyloxy)-1-hexene (5.17 g, 94%). Regioisomers could be separated by silica-gel chromatography.

4.1.2.1. (4R,5S)-2-[2-(Benzyloxy)ethyl]-5-fluoro-4,6-bis(triisopropylsilyloxy)-1-hexene (2).

^{19}F NMR (376 MHz, CDCl$_3$) δ −191.3 (dtd, $J = 45.5, 25.2, 23.7$ Hz, 1F); ^{1}H NMR (400 MHz, CDCl$_3$) δ 1.08 (bs, 42H), 2.35 (d, $J = 8.0$ Hz, 2H), 2.38 (t, $J = 6.8$ Hz, 2H), 3.60 (t, $J = 6.8$ Hz, 2H), 3.97 (dd, $J = 22.8, 4.8$ Hz, 2H), 4.34 (dtd, $J = 18.4, 8.0, 2.0$ Hz, 1H), 4.53 (s, 2H), 4.48–4.64 (dtd, $J = 48.0, 4.8, 2.0$ Hz, 1H), 4.92 (bs, 2H), 7.33–7.36 (m, 5H); ^{13}C NMR (101 MHz, CDCl$_3$) δ 12.0, 12.7, 18.0, 18.0, 18.1, 18.2, 36.4, 41.0 (d, $^3J = 8.4$ Hz), 62.1 (d, $^2J = 25.4$ Hz), 68.9, 71.5 (d, $^2J = 20.6$ Hz), 73.1, 96.3 (d, $^1J = 177.0$ Hz), 114.0, 127.6, 127.7, 128.4, 138.4, 142.6; IR (neat) 2946, 2870, 1647, 1464, 1383, 1365, 1249, 1102, 1069, 1015, 998, 907, 894, 797, 735, 683 cm^{-1}.

4.1.2.2. (4S, 5R)-2-[2-(Benzyloxy)ethyl]-4-fluoro-5,6-bis(triisopropylsilyloxy)-1-hexene.

^{19}F NMR (376 MHz, CDCl$_3$) δ −188.5 (ddt, $J = 46.6, 41.0, 15.0$ Hz, 1F); ^{1}H NMR (400 MHz, CDCl$_3$) δ 1.07–1.09 (m, 42H), 2.39 (ddd, $J = 34.0, 14.8, 6.8$ Hz, 1H), 2.48 (t, $J = 7.2$ Hz, 2H), 2.64 (ddd, $J = 25.2, 14.8, 10.0$ Hz, 1H), 3.65 (t, $J = 7.2$ Hz, 2H), 3.80–3.85 (m, 2H), 4.20–4.28 (m, 1H), 4.53 (s, 2H), 4.84–4.99 (ddt, $J = 43.2, 10.4, 2.0$ Hz, 1H), 4.97 (bs, 1H), 5.00 (bs, 1H), 7.30–7.37 (m, 5H); ^{13}C NMR (101 MHz, CDCl$_3$) δ 11.9, 12.6, 18.0, 18.1, 18.2, 35.2, (d, $^2J = 22.2$ Hz), 36.3, 64.5 (d, $^3J = 9.9$ Hz), 68.9, 72.3, 74.6 (d, $^2J = 20.7$ Hz), 93.3 (d, $^1J = 173.8$ Hz), 113.4, 127.6, 127.8, 128.4, 138.6, 143.0.

4.1.3. (2S,3R)-5-[2-(Benzyloxy)ethyl]-2-fluoro-3-triisopropylsilyloxy-5-hexen-1-ol (3)

To a solution of triethylamine (0.28 mL, 2.0 mmol) and HF/Py (0.048 mL, 2.0 mmol) in THF (2.5 mL) was added (4R,5S)-2-[2-(benzyloxy)ethyl]-5-fluoro-4,6-bis(triisopropylsilyloxy)-1-hexene (**2**) (0.240 g, 0.413 mmol) at 0 °C. After stirring for 22 h at room temperature, methoxytrimethylsilane (TMSOMe, 0.5 mL) was added to the reaction mixture at 0 °C and stirred for 2 h. After THF was evaporated under reduced pressure, the residue was purified by silica-gel chromatography to give (2S,3R)-5-[2-(benzyloxy)ethyl]-2-fluoro-3-triisopropylsilyloxy-5-hexen-1-ol (**3**) (0.116 g, 66%): ^{19}F NMR (376 MHz, CDCl$_3$) δ −193.3 (dddd, $J = 50.4, 39.9, 26.3, 14.7$ Hz, 1F); ^{1}H NMR (400 MHz, CDCl$_3$) δ 1.08 (bs, 21H), 1.61 (br, 1H) 2.30 (dd, $J = 14.8, 10.0$ Hz, 1H), 2.35 (t, $J = 6.8$ Hz, 2H), 2.44 (dd, $J = 14.8, 6.8$ Hz, 1H), 3.58 (t, $J = 6.8$ Hz, 2H), 3.88 (bdd, $J = 26.0, 12.4$ Hz, 1H), 4.01 (ddd, $J = 24.4, 12.4, 6.0$ Hz, 1H), 4.41 (dddd, $J = 17.6, 12.4, 5.2, 2.4$ Hz 1H), 4.43–4.58 (dtd, $J = 47.2, 6.0, 2.4$ Hz, 1H), 4.51 (s, 2H), 4.89 (bs, 1H), 4.91 (bs, 1H), 7.29–7.35 (m, 5H); ^{13}C NMR (101 MHz, CDCl$_3$) δ 12.5, 18.0, 36.1, 41.6 (d, $^3J = 9.2$ Hz), 61.3 (d, $^2J = 22.1$ Hz), 68.8, 72.0 (d, $^2J = 20.6$ Hz), 73.0, 94.7 (d, $^1J = 175$ Hz), 114.2, 127.6, 127.7, 128.3, 138.2, 142.1; IR (neat) 3350, 2946, 2868, 1647, 1497, 1456, 1365, 1249, 1207, 1100, 1067, 1015, 998, 884, 737, 681 cm^{-1}; $[\alpha_D^{24}] = -4.36$ (*ca.* 1.28, CHCl$_3$).

4.1.4. (2R,3R)-5-[2-(Benzyloxy)ethyl]-2-fluoro-3-triisopropylsilyloxy-5-hexenal (4)

To a suspension of powdered molecular sieves 3 Å (MS 3 Å, 3.0 g) and pyridinium chlorochromate (1.30 g, 6.0 mmol) in CH$_2$Cl$_2$ (60 mL) was added (2S,3R)-5-[2-(benzyloxy)ethyl]-2-fluoro-3-triisopropylsilyloxy-5-hexen-1-ol (**3**) (1.28 g, 3.02 mmol) in CH$_2$Cl$_2$ (3.0 mL) in the water bath. After stirring for 1 h, ether, celite and florisil were added and stirred for 10 min. Then the resultant suspension was filtered through a column of celite and florisil. After evaporation under reduced pressure, the resultant residue was purified by silica-gel chromatography to give (2R,3R)-5-[2-(benzyloxy)ethyl]-2-fluoro-3-triisopropylsilyloxy-5-hexenal (1.02 g, 80%): ^{19}F NMR (376 MHz, CDCl$_3$) δ −206.2 (ddd, $J = 49.3, 21.8, 3.8$ Hz, 1F); ^{1}H NMR (300 MHz, CDCl$_3$); δ 1.08 (bs, 21H), 2.30 (d, $J = 6.4$Hz, 2H), 2.40 (d, $J = 14.4$ Hz, 1H), 2.57 (dd, $J = 14.4, 10.8$ Hz, 1H), 3.58 (t, $J = 6.4$ Hz, 2H), 4.45–4.54 (m, 1H), 4.51 (s, 2H), 4.76 (d, $J = 48.8$ Hz, 1H), 5.01 (s, 1H), 7.32–7.35 (m, 5H), 9.70 (d, $J = 5.2$ Hz, 1H); ^{13}C NMR (75 MHz, CDCl$_3$) δ 12.2, 17.8, 17.9, 36.0, 40.1, 68.5, 72.9, 73.6 (d, $^2J = 19.2$ Hz), 96.3 (d, $^1J = 185$ Hz), 115.6, 127.5, 127.5, 127.5, 127.6, 128.3, 138.2, 147.8, 198.9 (d, $^2J = 37.5$ Hz); IR (neat) 2948, 2870, 1744, 1647, 1458, 1363, 1114, 1000, 884, 735 cm^{-1}; $[\alpha_D^{24}] = +17.6$ (*ca.* 1.87, CHCl$_3$).

4.1.5. (Z,1R,2S,3R)-5-[2-(Benzyloxy)ethylidene]-2-fluoro-3-triisopropylsilyloxy-1-cyclohexanol. (trans, Z-exo) (5)

To a solution of (R)-BINOL-derived chiral titanium complex [34,35] (0.0251 g, 0.045 mmol) in CH_2Cl_2 (2.5 mL) was added (2R,3R)-5-[2-(benzyloxy)ethyl]-2-fluoro-3-(triisopropylsily-loxy)-5-hexenal (4) (0.189 g, 0.45 mmol) at room temperature under an argon atmosphere. After stirring for 24 h at that temperature, the reaction mixture was poured into sat. sodium hydrogencarbonate. After usual workup, the residue was purified by silica-gel chromatography to give trans,Z-exo, trans,E-exo, cis-endo, trans-endo, cis-exo (E/Z mixture) (0.132 g, 94%) as regioisomers in a ratio of 71:8:11:6:3. (Z,1R,2S,3R)-5-[2-(Benzyloxy)ethylidene]-2-fluoro-3-triiso-propylsilyloxy-1-cyclohexanol (trans,Z-exo) (5) was separated by silica-gel chromatography: ^{19}F NMR (376 MHz, CDCl$_3$); δ −192.4 (cis-exo, m, 1F), −195.3 (cis-exo, m, 1F), −197.8 (trans,Z-exo, bd, J = 43.6 Hz, 1F), −198.9 (trans,E-exo, bd, J = 45.9 Hz, 1F), −199.9 (trans-endo, bd, J = 44.1 Hz, 1F), −202.9 (cis-endo, bd, J = 50.4 Hz, 1F); ^{1}H NMR (400 MHz, CDCl$_3$) δ 1.04 (bs, 21H), 2.15 (d, J = 13.5 Hz, 2H), 2.55–2.66 (m, 2H), 4.02 (dd, J = 11.7, 6.6 Hz, 2H), 4.11–4.17 (m, 2H), 4.27 (d, J = 6.3 Hz, 1H), 4.38 (ddd, J = 34.5, 7.8, 3.0 Hz, 1H), 4.49 (s, 2H), 5.61 (t, J = 6.6 Hz, 1H), 7.33–7.35 (m, 5H); ^{13}C NMR (101 MHz, CDCl$_3$) δ 12.2, 17.8, 17.9, 33.6 (d, ^{3}J = 5.4 Hz), 40.4 (d, ^{3}J = 5.4 Hz), 65.9, 67.9 (d, ^{2}J = 21.4 Hz), 68.8 (d, ^{2}J = 16.9 Hz), 72.2, 95.7 (d, ^{1}J = 184 Hz), 124.2, 127.5, 127.7, 128.2, 135.5, 137.9; IR (neat) 3302, 3034, 2946, 2868, 1497, 1464, 1383, 1365, 1249, 1187, 1123, 1067, 1027, 998, 917, 882, 750, 698, 679 cm^{-1}; [α$_D$^{27}] = +7.70 (ca. 0.71, CHCl$_3$); HPLC (Inertsil SIL, hexane/ethyl acetate = 4:1, flow rate 0.8 mL/min, detection 254 nm light); trans,Z-exo t_R = 18.4 min; trans-endo t_R = 15.6 min; trans,E-exo t_R = 15.0 min; cis-endo t_R = 14.3 min; cis-exo t_R = 13.9 min; cis-exo t_R = 9.4 min.

4.1.6. (Z,1S,2R,6R)-4-[2-(Benzyloxy)ethylidene]-1-fluoro-2,6-bis(triisopropylsilyloxy)cyclohexane (6)

To a solution of (1R,2S,3R)-5-[(Z)-2-(benzyloxy)ethyli-dene]-2-fluoro-3-(triisopropylsilyloxy)-cyclohexanol (5) (0.372 g, 0.880 mmol) in CH_2Cl_2 (0.88 mL) was added 2,6-lutidine (0.26 mL, 2.20 mmol) and triisopropylsilyltriflate (TIPSOTf) (0.31 mL, 1.14 mmol) at 0 °C. After stirring for 1 h at that temperature, the reaction mixture was quenched with sat. sodium hydrogencarbonate. After usual workup, the resultant residue was purified by silica-gel chromatography to give (1R,2S,3R)-5-[(Z)-2-(benzyloxy)ethylidene]-2-fluoro-1,3-bis(triisopropylsilyloxy)-cyclohexane (6) (0.510 g, 100%): ^{19}F NMR (376 MHz, CDCl$_3$) δ −199.5 (bs, 1F); ^{1}H NMR (400 MHz, CDCl$_3$) δ 1.05 (bs, 42H), 2.16 (dd, J = 14.0, 6.0 Hz, 1H), 2.36 (dd, J = 14.0, 4.4 Hz, 1H), 2.40 (dd, J = 14.0, 4.8 Hz, 1H), 2.53 (dt, J = 14.0, 4.4 Hz, 1H), 4.05 (d, J = 6.8 Hz, 2H), 4.19 (dddd, J = 21.2, 7.2, 4.4, 2.4 Hz, 1H), 4.25 (ddt, J = 12.0, 6.0, 4.4 Hz, 1H), 4.46 (ddd, J = 49.6, 6.0, 2.4 Hz, 1H), 4.46 (d, J = 12.0 Hz, 1H), 4.50 (d, J = 12.0 Hz, 1H), 5.51 (t, J = 6.8 Hz, 1H), 7.28–7.35 (m, 5H); ^{13}C NMR (101 MHz, CDCl$_3$) δ 12.2, 12.2, 12.3, 17.7, 17.9, 33.1 (d, ^{3}J = 5.4 Hz), 40.5, 65.9, 68.9 (d, ^{2}J = 16.9 Hz), 69.2 (d, ^{2}J = 23.7 Hz), 71.9, 94.3 (d,

^{1}J = 184 Hz), 123.5, 127.5, 127.7, 128.3, 136.3, 138.3; IR (neat) 2945, 2896, 2868, 1464, 1383, 1367, 1249, 1112, 1069, 1013, 998, 917, 884, 795, 758, 679 cm^{-1}; [α$_D$^{27}] = −9.49 (ca. 1.21, CHCl$_3$).

4.1.7. (Z,3R,4S,5R)-2-[4-Fluoro-3,5-bis(triisopropylsilyloxy)cyclohexylidene]ethanol (7)

A 25 mL, three necked, round-bottomed flask equipped with a finger-type-condenser and a magnetic stirring bar and argon inlet was charged with anhydrous liquid ammonia (ca. 0.18 mL) at −78 °C. To the solution were added lumps of lithium (ca. 0.049 g, 7.0 mmol) and then (1R,2S,3R)-5-[(Z)-2-(benzyloxy)ethylidene]-2-fluoro-1,3-bis(triisopropylsilyloxy)-cyclohexane (6) (0.510 g, 0.880 mmol) in ether (0.88 mL) and tert-butyl alcohol (0.33 mL) at that temperature. After stirring for 15 min, methanol (1.0 mL) was added to the reaction mixture. Then the mixture was warmed up to room temperature until the excess ammonium evaporated. After usual workup, the resultant residue was purified by silica-gel chromatography to give (Z,3R,4S,5R)-2-[4-fluoro-3,5-bis(triisopropylsilyloxy)cy-clohexylidene]-ethanol (7) (0.364 g, 85%): ^{19}F NMR (376 MHz, CDCl$_3$) δ −198.6 (bs, 1F); ^{1}H NMR (300 MHz, CDCl$_3$) δ 1.05 (bs, 3H), 1.06 (bs, 3H), 1.07 (bs, 18H), 1.07 (bs, 18H), 1.24 (bs, 1H), 2.13 (dd, J = 13.8, 6.3 Hz, 1H), 2.36 (dd, J = 13.8, 3.9 Hz, 1H), 2.45–2.55 (bd, J = 13.8 Hz, 1H), 2.50 (dd, J = 13.8, 3.9 Hz, 1H), 4.13 (dd, J = 12.0, 6.9 Hz, 1H), 4.18 (dd, J = 12.0, 6.9 Hz, 1H), 4.19–4.27 (m, 2H), 4.29–4.54 (ddd, J = 49.5, 6.3, 2.4 Hz, 1H), 5.54 (t, J = 6.9 Hz, 1H); ^{13}C NMR (75 MHz, CDCl$_3$) δ 12.1, 12.2, 17.8, 33.0 (d, ^{3}J = 6.1 Hz), 40.8 (d, ^{3}J = 3.7 Hz), 69.1 (d, ^{2}J = 16.9 Hz), 69.3 (d, ^{2}J = 23.1 Hz), 94.7 (d, ^{1}J = 183 Hz), 126.4, 135.9; IR (neat) 3242, 2948, 2896, 2870, 2362, 1464, 1383, 1247, 1118, 1071, 1041, 998, 917, 884, 758, 679 cm^{-1}; [α$_D$^{27}] = −3.55 (ca. 1.26, CHCl$_3$).

4.1.8. (Z,1S,2R,6R)-4-[2-Chloroethylidene]-1-fluoro-2,6-bis(triisopropylsilyloxy)cyclohexane (8)

To a solution of N-chlorosuccimide (0.116 g, 0.87 mmol) in CH_2Cl_2 (1.8 mL) was slowly added dimethyl sulfide (0.068 mL, 0.92 mmol) at 0 °C under argon. After stirring for 10 min at that temperature, then mixture was cooled to −20 °C for 10 min, and a solution of 2-[(3R,4S,5R)-4-fluoro-3,5-bis(triisopropylsilylox-y)cyclohexylidene]ethanol (7) (0.089 g, 0.181 mmol) in CH_2Cl_2 (1.0 mL) was added. After stirring for 15 min at that temperature, the mixture was warmed up to room temperature for 1.5 h. After usual workup, the residue obtained was purified by neutral silica-gel chromatography to give (Z,1S,2R,6R)-4-[2-chloroethy-lidene]-1-fluoro-2,6-bis(triisopropylsilyloxy)cyclohexane (8) (0.070 g, 76%): ^{19}F NMR (376 MHz, CDCl$_3$) δ −200.0 (m, 1F); ^{1}H NMR (300 MHz, CDCl$_3$) δ 1.08 (bs, 42H), 2.16 (dd, J = 14.0, 5.2 Hz, 1H), 2.45 (d, J = 6.0 Hz, 2H), 2.51 (dt, J = 14.0, 4.4 Hz, 1H), 4.04 (dd, J = 11.6, 7.6 Hz, 1H), 4.13 (dd, J = 11.6, 8.0 Hz, 1H), 4.20–4.28 (m, 2H), 4.42–4.56 (ddd, J = 49.2, 5.6, 2.0 Hz, 1H), 5.54 (t, J = 8.0 Hz, 1H).; ^{13}C NMR (75 MHz, CDCl$_3$) δ 12.2, 12.4, 18.0, 18.0, 18.0, 31.7 (d, ^{3}J = 5.4 Hz), 39.9, 40.2, 68.8 (d, ^{2}J = 17.7 Hz), 69.1 (d, ^{2}J = 24.5 Hz), 94.0 (d, ^{1}J = 184 Hz), 122.7, 138.3; IR (neat) 2948, 2870, 1464, 1386,

1253, 1127, 1038, 1015, 998, 917, 884, 760, 681 cm^{-1}; [α_D^{27}] = +12.9 (*ca.* 1.36, CHCl$_3$).

4.1.9. (Z,1S,2R,6R)-1-Fluoro-4-[2-(diphenylphosphinyl)ethylidene]-2,6-bis(triisopropylsilyloxy)cyclohexane (9)

To a solution of (Z,1S,2R,6R)-4-[2-chloroethylidene]-1-fluoro-2,6-bis(triisopropylsilyloxy)cyclohexane (**8**) (0.100 g, 0.197 mmol) in THF (1.9 mL) was slowly added a freshly prepared THF solution of lithium diphenylphosphide, until a yellow color persisted at −78 °C under an argon. This was quenched with water (0.8 mL), and the reaction mixture was warmed up to room temperature. After THF was evaporated under reduced pressure, the gummy residue was dissolved in CH$_2$Cl$_2$ (4.0 mL), 12 drops of 30% hydrogen peroxide were added and then stirred for 1 h at room temperature. After usual workup, the resultant residue was purified by silica-gel chromatography to give (Z,1S,2R,6R)-1-fluoro-4-[2-(diphenyl-phosphinyl)ethylidene]-2,6-bis(triisopropylsilyloxy)cyclohexane (**9**) (0.117 g, 88%): ^{19}F NMR (376 MHz, CDCl$_3$) δ −199.1 (bs, 1F); ^{1}H NMR (400 MHz, CDCl$_3$) δ 1.01 (bs, 6H), 1.06 (bs, 36H), 2.01 (bd, J = 10.8 Hz, 1H), 2.08 (bd, J = 10.8 Hz, 1H), 2.40–2.45 (m, 2H), 3.13 (dd, J = 14.8, 7.6 Hz, 2H), 4.07–4.20 (m, 2H), 4.31–4.45 (ddd, J = 49.6, 6.0, 2.0 Hz, 1H), 5.38 (dd, J = 14.0, 7.2 Hz, 1H), 7.46 (td, J = 7.6, 2.0 Hz, 2H), 7.53 (bt, J = 7.6 Hz, 4H), 7.71 (dd, J = 11.2, 7.6 Hz, 4H); ^{13}C NMR (101 MHz, CDCl$_3$) δ 12.2, 12.3, 12.3, 12.4, 18.0, 18.0, 30.5 (d, $^1J_{\text{C-P}}$ = 70.4 Hz), 33.0, 40.7, 68.7 (d, $^2J_{\text{C-F}}$ = 16.8 Hz), 69.6 (d, $^2J_{\text{C-F}}$ = 21.4 Hz), 94.3 (d, $^1J_{\text{C-F}}$ = 185 Hz), 114.6(d, $^2J_{\text{C-P}}$ = 9.2 Hz), 128.5 (d, $^3J_{\text{C-P}}$ = 2.3 Hz), 128.6 (d, $^3J_{\text{C-P}}$ = 2.3 Hz), 130.9 (d, $^2J_{\text{C-P}}$ = 8.5 Hz), 131.1 (d, $^2J_{\text{C-P}}$ = 8.4 Hz), 131.8 (d, $^4J_{\text{C-P}}$ = 3.1 Hz), 131.9 (d, $^4J_{\text{C-P}}$ = 3.1 Hz), 132.3 (d, $^1J_{\text{C-P}}$ = 98.8 Hz), 132.9 (d, $^1J_{\text{C-P}}$ = 98.8 Hz), 137.1 (d, $^3J_{\text{C-P}}$ = 11.5 Hz); IR(neat) 2948, 2868, 1464, 1439, 1386, 1245, 1193, 1120, 1071, 1015, 998, 971, 917, 884, 851, 828, 754, 719, 683, 661 cm^{-1}; [α_D^{27}] = −12.7 (*ca.* 1.52, CHCl$_3$).

4.1.10. 2α-Fluoro-19-nor-1α,3β-bis(triisopropylsilyloxy)-25-(trimethylsilyloxy)-22-oxavitamin D$_3$

A solution of (Z,1S,2R,6R)-1-fluoro-4-[2-(diphenylphosphinyl)ethylidene]-2,6-bis(triisopropylsilyloxy)cyclohexane (**9**) (0.064 g, 0.095 mmol) in THF (1.9 mL) was cooled at −78 °C and treated dropwise with 2.0 M *n*-butyllithium in pentane (0.050 mL, 0.099 mmol) under an argon. After stirring for 5 min, a solution of de-A,B-8-oxo-25-(trimethylsilyloxy)-22-oxacholestane (0.037 g, 0.104 mmol) in THF (0.6 mL) was added dropwise to the resultant deep red solution at −78 °C over 10 min. The reaction mixture was gradually warmed up to room temperature over about 20 h in the dark with stirring. After the addition of a 2 N sodium potassium tartrate (0.6 mL) and a 2 N potassium bicarbonate (0.6 mL), the reaction mixture was extracted three times with ethyl acetate. The combined organic layers were washed with brine and dried over anhydrous sodium sulfate. After evaporation under reduced pressure, the resultant residue was purified by neutral silica-gel chromatography to give 2α-fluoro-19-nor-1α,3β-bis(triisopropylsilyloxy)-25-(trimethylsilyloxy)-22-oxavitamin D$_3$

(0.025 g, 33%): ^{19}F NMR (376 MHz, CDCl$_3$) δ −197.7 (bs, 1F); ^{1}H NMR (300 MHz, CDCl$_3$) δ 0.10 (s, 9H), 0.53 (s, 3H), 1.04 (bs, 6H), 1.05 (bs, 18H), 1.06 (bs, 18H), 1.16 (d, J = 6.0 Hz, 3H), 1.50–1.57 (m, 7H), 1.60–1.64 (m, 2H), 1.66–1.74 (td, J = 10.5, 2.1 Hz, 1H), 1.88 (bd, J = 11.7 Hz, 1H), 1.99 (m, 2H), 2.15 (dd, J = 14.1, 6.6 Hz, 1H), 2.39 (d, J = 14.4, 2.0 Hz, 1H), 2.40–2.64 (m, 2H), 2.77 (dd, J = 12.9, 3.9 Hz, 1H), 3.21 (bt, J = 6.3 Hz, 1H), 3.33 (bq, J = 6.3 Hz, 1H), 3.65 (bq, J = 6.3 Hz, 1H), 4.17–4.27 (m, 2H), 4.32–4.50 (ddd, J = 49.2, 7.4, 2.1 Hz, 1H), 5.82 (d, J = 10.8 Hz, 1H), 6.19 (d, J = 11.1 Hz, 1H); ^{13}C NMR (75 MHz, CDCl$_3$) δ 2.4, 12.2, 12.5, 17.9, 17.9, 19.2, 22.0, 23.1, 25.6, 30.3, 33.1, 39.7, 41.8, 44.5 (d, ^3J = 2.5 Hz), 56.2, 57.4, 65.0, 69.4 (d, ^2J = 17.0 Hz), 69.6 (d, ^2J = 21.8 Hz), 73.2, 78.1, 95.5 (d, ^1J = 184 Hz), 116.5, 122.9, 131.6, 141.5; IR (neat) 2948, 2870, 1464, 1381, 1367, 1325, 1251, 1218, 1112, 1038, 998, 967, 917, 884, 859, 839, 804, 758, 710, 681 cm^{-1}; [α_D^{27}] = +33.7 (*ca.* 1.26, CHCl$_3$).

4.1.11. 2α-Fluoro-19-nor-1α,25-dihydroxy-22-oxavitamin D$_3$ (10)

To a solution of 2α-fluoro-19-nor-1α,3β-bis(triisopropylsilyloxy)-25-(trimethylsilyloxy)-22-oxavitamin D$_3$ (0.0025 g, 0.031 mmol) in THF (3.1 mL) was added a 1 M solution of tetrabutylammonium fluoride (TBAF) in THF (0.31 mL, 3.1 mmol) at room temperature. After stirring for 24 h at that temperature, the solution was evaporated under reduced pressure. The residue was purified by neutral silica-gel chromatography to give 2α-fluoro-19-nor-1α,25-dihydroxy-22-oxavitamin D$_3$ (**10**) (0.012 g, 92%): ^{19}F NMR (376 MHz, CDCl$_3$) δ −201.0 (bd, J = 45.9 Hz, 1F); ^{1}H NMR (400 MHz, CDCl$_3$) δ 0.54 (s, 3H), 1.19 (d, J = 6.0 Hz, 3H), 1.23 (s, 3H), 1.24 (s, 3H), 1.56–1.60 (m, 11H), 1.86–1.89 (m, 1H), 1.96–2.02 (m, 2H), 2.17–2.22 (m, 1H), 2.36–2.39 (m, 1H), 2.62–2.72 (m, 1H), 2.78–2.82 (m, 1H), 3.24–3.27 (m, 1H), 3.46–3.51 (m, 1H), 3.82–3.87 (m, 1H), 4.09–4.23 (m, 2H), 4.49 (ddd, J = 49.6, 7.2, 2.8 Hz, 1H), 5.82 (d, J = 11.2 Hz, 1H), 6.35 (d, J = 11.2 Hz, 1H); ^{13}C NMR (75 MHz, CDCl$_3$) δ 12.6, 18.7, 22.1, 23.0, 25.7, 28.7, 29.0, 29.2, 32.2, 39.5, 40.5 (d, ^3J = 4.8 Hz), 41.4, 44.7, 56.1, 57.1, 65.6, 68.2 (d, ^2J = 18.2 Hz), 68.5 (d, ^2J = 21.8 Hz), 70.6, 79.0, 96.0 (d, ^1J = 177 Hz), 115.9, 124.8, 129.4, 143.3; IR (neat) 3320, 3052, 2936, 2878, 1622, 1446, 1379, 1348, 1267, 1154, 1081, 1019, 965, 897, 866, 828, 795, 737, 702 cm^{-1}; [α_D^{26}] = +80.1 (*ca.* 0.87, CHCl$_3$); HRMS *m/z* calcd. for C$_{25}$H$_{41}$FO$_4$ (M$^+$) 424.4989, found 424.3004.

4.2. Cell culture

Human promyelocytic leukemia HL-60 cells were obtained from Dr. Y. Seino of the Okayama University School of Medicine. The cells were maintained in continuous culture in RPMI-1640 medium (Nissui Seiyaku Co. Ltd., Tokyo, Japan) supplemented with 10% fetal bovine serum (Gibco BRL, Grand Island, NY, USA), 0.06 mg/mL kanamycin (Sigma).

Human osteosarcoma MG-63 cells, were maintained in Dulbecco's modification Eagle medium (Gibco BRL) supplemented with 1% penicillin, 1% streptomycin and 10% dextran-coated charcoal-treated fetal calf serum (Gibco BRL).

Cloned metastatic variant cells of Lewis lung carcinoma (LLC) were kindly supplied by the Cell Resource Center for Biomedical Research, Tohoku University. We previously generated the GFP expression vector stable transfected LLC cells (LLC-GFP cells) [21]. The medium used for culturing the tumor cells and for all assays was RPMI1640 medium (Life Technologies, Grand Island, NY) supplemented with L-glutamine (0.29 mg/mL), kanamycin (0.06 mg/mL) and 10% heat-inactive fetal bovine serum.

4.3. HL-60 cells and synchronization of cell cycle at S phase by excess amounts of thymidine

HL-60 cells were synchronized at S phase by the following procedure: Cells (4×10^5 cells/mL) were cultured in 30 mL of RPMI-1640 medium for 24 h and subsequently cultured for 16 h in RPMI-1640 medium supplemented with 2.5 mM thymidine. After washing the cells with Ca, Mg-free phosphate buffered saline [PBS(−)] twice, the synchronization of cell cycle by the same manner was repeated, and the cells thus obtained were used in the following experiments.

4.4. Flow cytometry

Cells (10^5 cells/well) were placed in 24-well tissue culture plates and cultured for 3 days in RPMI-1640 medium with $1\alpha,25$-D_3 or analogs under the same conditions as above. To reduce the effects of contact inhibition, control cells were adjusted to 60–70% confluence at the time of FACS analysis. Each group of cells was collected and washed with PBS(−) once. Then, the cells were resuspended in PBS(−) containing 0.2% Triton-X and 100 µg RNase, and incubated at 37 °C for 1 h. Cells were washed with PBS(−) and incubated with 0.5 mL of DNA-staining solution containing propidium iodide (50 µg/mL) at 4 °C for 20 min. The cells were analyzed with a flow cytometer equipped with an argon laser (488 nm, Becton Dickinson FACScan™) and cell cycle distribution was analyzed by ModiFiT LT(Verity). Experiments were repeated three times.

4.5. Cell surface antigen expression analysis

Cells (10^5 cells/well) were placed in 24-well tissue culture plates, and cultured for 3 days in RPMI-1640 medium with $1\alpha,25$-D_3 or analogs under the same conditions as above. Each group of cells was then collected and washed with PBS(−) once. Then, the cells (2×10^5 cells) were resuspended in 100 µL diluent solution containing 1% bovine serum albumin (BSA) and 1% sodium azide and incubated with 10 µL human monoclonal FITC conjugated CD11b antibody (Sigma, USA) and 10 µL human monoclonal PE conjugated CD14 antibody (Sigma, USA) for 30 min at room temperature without light. The cells were washed once with diluent solution and then fixed in 300 µL of PBS(−) containing 2% paraformaldehyde. Fluorescence was detected on a Becton Dickinson FACScan™ at excitation wavelength of 490 nm and emission wavelength of 520 nm. Results were recorded as the mean fluorescence index,

which is the product of the % fluorescence and the mean fluorescence intensity, with 10^4 cells counted per treatment.

4.6. Transfection and luciferase activity assay

MG-63 cells, which are positive for VDR and RXR gene expression, were transfected with 0.5 µg luciferase reporter plasmid (pGVB2 vector, Toyo Ink Co., Ltd., Tokyo, Japan) inserted with a rat 25(OH)D_3-24-hydroxylase gene promoter (−291/+9) including the two VDREs [49] and 0.25 µg of the pRL-CMV vector (Toyo Ink Co., Ltd.) as an internal control using the Tfx-50 reagent (Promega Corp., Tokyo, Japan). In the mammalian two-hybrid luciferase assay, MG-63 cells were transfected with 0.5 µg of a pM vector containing a human RXRα cDNA connected to GAL-DBD (pM-RXRα) or containing a steroid receptor coactivator-1 (SRC-1) [50] cDNA connected to GAL-DBD (pM-SRC-1), 0.5 µg of a pVP16 vector (CLONTECH) containing a human VDR cDNA connected to VP16 transactivation domain (pVP16-hVDR), 0.5 µg of pGVP2 vector containing GAL-BS and a pRL-CMV vector as an internal control using the Tfx-50 reagent. The cells were incubated with various concentrations of $1\alpha,25$-D_3 or its analogs for 2 days. The luciferase activities of the cell lysates were measured with a luciferase assay system (Toyo Ink Co., Ltd.), according to the manufacturer's instructions. Transactivation measured by luciferase activity was standardized with the luciferase activity of the same cells determined by the Sea Pansy luciferase assay system as a control (Toyo Ink Co., Ltd.). Each set of experiments was repeated at least three times, and the results are presented in terms of fold-induction as means ± S.E.

4.7. Animals

Female C57BL/6J mice (Clea Japan, Inc., Tokyo, Japan), 10 weeks of age, were used for all experiments. Mice were then fed *ad libitum* distilled water and a chow diet (F-2, Clea Japan, Inc., Tokyo, Japan; ingredients: 1.2% calcium, 0.6% phosphorus and 1.08 IU vitamin D_3/g). The mice were maintained under specific pathogen-free conditions with a 12 h light, 12 h dark cycle. This study was conducted in accordance with the standards established by the Guidelines for the Care and Use of Laboratory Animals of Kobe Pharmaceutical University.

$VDR^{-/-}$ mice were generated by homologous gene targeting as described previously [44]. Null mutant mice were obtained by intercrossing a heterozygous VDR knockout female and a heterozygous male. Mice were weaned at 3 weeks of age and then fed *ad libitum* a high calcium and vitamin D-deficient diet (Clea Japan, Inc.; ingredients: 2% calcium, 1.25% phosphorus, 0 IU vitamin D_3/100 g, and 20% lactose). We used the wild-type ($VDR^{+/+}$) and $VDR^{-/-}$ mice, 10 weeks of age.

4.8. In vivo calcium-regulating assay

Ten week-old normal C57BL/6J female mice were divided into several groups of six mice, each receiving oral administration of 1, 10 or 100 µg/kg of $1\alpha,25$-D_3 or its analogs in

2 μL/kg of 0.1% Triton X-100 solution. The resulting increases in serum calcium were measured at 8, 24, 48 and 72 h after administration by the *o*-cresolphthalein complexone (OCPC) method. The relative activity of each analog with respect to $1\alpha,25\text{-D}_3$ was evaluated as follows: the dose–response effect of each analogue was calculated at the time when the effect was maximum and expressed as the dosage required to elevate the serum calcium level by 1 mg/dL.

4.9. Assessment of cell growth in vitro in LLC-GFP cells

The effects of $2\alpha\text{-F-19-nor-22-oxa-}1\alpha,25\text{-D}_3$ and $1\alpha,25\text{-D}_3$ on the proliferation of LLC-GFP cells *in vitro* were assessed by cell counting and cell cycle analysis. Cells were seeded at a density of 2×10^5 cells/well in 6-well culture plates in RPMI1640 medium containing 10% fetal bovine serum for 24 h. After 24 h, fresh medium containing 10% FBS with vehicle (ethanol), $1\alpha,25\text{-D}_3$ or $2\alpha\text{-F-19-nor-22-oxa-}1\alpha,25\text{-D}_3$ (10^{-7} M) was added to cultured cells, and incubation continued for 3 days. $1\alpha,25\text{-D}_3$ and $2\alpha\text{F-19-nor-22-oxa-}1\alpha,25\text{-D}_3$ were dissolved in ethanol, the final concentration of ethanol in all cultures not exceeding 0.1%. Cells were trypsinized at specific time points, and an aliquot of cells was counted and the cell cycle analyzed. For the analysis of the cell cycle, each group of cells was collected and washed with PBS (−) once. Then the cells were resuspended in PBS (−) containing 0.2% Triton-X and 100 μg of RNase and incubated at 37 °C for 30 min. Cells were washed with PBS (−) and incubated with 0.5 mL of DNA-attaining solution containing propidium iodide (50 μg/mL) at 4 °C for 20 min. The cells were analyzed with a flow cytometer equipped with an argon laser (488 nm, Becton Dickinson FACScan™) and the cell cycle distribution was analyzed using ModiFit LT (Verity).

4.10. In vitro invasion of LLC-GFP cells through a Matrigel-coated membrane

The capacity of tumor cells to traverse a basement membrane-matrix-coated filter has been shown to be representative of their invasiveness. Therefore, the capacity of tumor cells to migrate through Matrigel-coated membranes was measured. Nucleopore filters (8 μm pore size) were coated with 100 μL of a 1:20 dilution of Matrigel (Becton Dickinson, Bedford, MA) and allowed to dry. Representative filters were stained with crystal violet and, when examined microscopically, appeared to be evenly coated with Matrigel. Medium was added to the lower compartment of each blind-well chemotactic chamber. A dried, coated filter was placed over the lower compartment. After reconstitution of Matrigel, 5×10^4 cells were added to the upper compartment together with the same concentration of $1\alpha,25\text{-D}_3$ or $2\alpha\text{-F-19-nor-22-oxa-}1\alpha,25\text{-D}_3$ with which the cells had been preincubated with vehicle, $1\alpha,25\text{-}$ D_3 or $2\alpha\text{-F-19-nor-22-oxa-}1\alpha,25\text{-D}_3$ (10^{-8} or 10^{-7} M) for 3 days. Chambers were incubated for 24 h, after which filters were removed, wiped clean on the upper surface and fixed in 10% formalin. The number of cells on the lower surface of the filter was counted under the fluorescent microscope. Data were

reported as the number of cells/low power field enumerated from triplicate chambers from each of four experiments.

4.11. Intravenous injection of LLC-GFP cells in VDR$^{-/-}$ mice with corrected hypocalcemia and hypervitaminosis D and administration of 2α-F-19-nor-22-oxa-$1\alpha,25$-D$_3$

$VDR^{-/-}$ mice were generated by homologous gene targeting as described previously [45]. Mice were weaned at 3 weeks of age then fed a high calcium and vitamin D-deficient diet (Clea Japan, Inc.; ingredients: 2% calcium, 1.25% phosphorus, 0 IU vitamin D_3/100 g, and 20% lactose) *ad libitum*. We used wild-type ($VDR^{+/+}$) and $VDR^{-/-}$ mice, 10 weeks of age, which were fed a high calcium and vitamin D-deficient diet to completely eliminate endogenous $1\alpha,25\text{-D}_3$ and to correct serum calcium levels. First, we confirmed that $VDR^{-/-}$ mice showed extreme hypervitaminosis D along with severe hypocalcemia when compared to $VDR^{+/+}$ mice. Feeding of the high calcium and vitamin D-deficient diet resulted in the complete elimination of $1\alpha,25\text{-D}_3$ both before and after $2\alpha\text{-F-19-nor-22-oxa-}1\alpha,25\text{-D}_3$ administration in $VDR^{+/+}$ and $VDR^{-/-}$ mice. Mice were injected *i.v.* with a single dose of 5×10^5 LLC-GFP cells in a total volume of 0.2 mL in RPMI1640 medium containing 10% FBS. Thereafter, $2\alpha\text{-F-19-nor-22-oxa-}1\alpha,25\text{-D}_3$ was administered continuously using an osmotic minipump (model 2 ML4 Alzet; Alza Corp., Palo Alto, CA) implanted s.c. on the same day as the inoculation with LLC-GFP cells. An infusion rate of 10 or 50 μg/kg/24 h was chosen, and each minipump contained $2\alpha\text{-F-19-nor-}$ $22\text{-oxa-}1\alpha,25\text{-D}_3$ dissolved in 0.1% Tween-20 and 10% ethanol to deliver a continuous dose for up to 3 weeks at a rate of 2.5 μL/h. Untreated animals were implanted with a minipump containing vehicle alone. Mice with tumor implants were sacrificed 3 weeks later and serum Ca level, lung weight, number of lung nodules and GFP mRNA expression in the lung were measured.

4.12. Imaging and tumor scoring

A Leica fluorescence stereomicroscope model MZ FL III (Leica Microsystem, Inc., USA) equipped with a mercury 50 W lamp power supply was used. Selective excitation of GFP was produced through a D480/40 band-pass filter and 510 DCXR dichroic mirror. Emitted fluorescence was collected through a long-pass filter DC300F and digital camera system (Leica Microsystem, Inc., USA). The numbers of metastatic nodules on the surface of the lung were counted under the fluorescence stereomicroscope. To quantify lung metastasis, the GFP-expressing spots on the lungs were enumerated.

4.13. Real-time quantitative PCR

Lung tissues and LLC-GFP cells were homogenized in ISOGEN (Nippon Gene, Tokyo Japan). Total RNA was isolated as specified by the manufacturer. The purified RNA was reverse-transcribed with AMV reverse transcriptase (TaKaRa, Japan). Quantitative analyses of gene expression were conducted using GFP (5′-CTGCTCTCTTGGGTCCACTGG-3′ and 5′-CACCGCCTTGGCTTGTCACAT-3′), and β-actin

(5′-AGGCCCAGAGCAAGAGAGGTAT-3′ and 5′-CATGTC-GTCCCAGTTGGTAACA-3′)-specific primer sets, a Gene-eAmp 5700 Sequence Detection System (PE Biosystems, Foster City, CA) and the SYBR Green core reagent kit (PE Biosystems, Foster City, CA).

4.14. Analysis of serum calcium level

The blood samples were centrifuged at $3000 \times g$ for 10 min and the supernatants were employed as serum samples. The serum calcium level was determined by micro colorimetric assay (Wako, Japan).

4.15. Statistical analyses

Data are presented as the mean ± S.E. Student's *t*-test or Turkey's test were used for group analyses. Correlation coefficients were calculated for possible interrelations between variables. *P* values < 0.05 were considered as statistically significant.

Acknowledgments

References

[1] M.F. Holick, H.K. Schnoes, H.F. Deluca, T. Suda, R.J. Cousins, Biochemistry 10 (1971) 2799–2804.
[2] P.P. Minghetti, A.W. Norman, FASEB J. 2 (1988) 3043–3053.
[3] M.R. Walters, Endocr. Rev. 13 (1992) 719–764.
[4] E. Abe, C. Miyaura, H. Sakagami, M. Takeda, K. Konno, T. Yamazaki, S. Yoshiki, T. Suda, Proc. Natl. Acad. Sci. USA 78 (1981) 4990–4994.
[5] J.W. Pike, Annu. Rev. Nutr. 11 (1991) 189–216.
[6] R.M. Evans, Science 240 (1988) 889–895.
[7] K. Umesono, K.K. Murakami, C.C. Thompson, R.M. Evans, Cell 65 (1991) 1255–1266.
[8] J. Liao, K. Ozono, T. Sone, D.P. McDonnel, J.W. Pike, Proc. Natl. Acad. Sci. USA 87 (1990) 9751–9755.
[9] M.J. Tsai, B.W. O'Malley, Annu. Rev. Biochem. 63 (1994) 451–486.
[10] G.M. Palmieri, J. Clin. Endocrinol. Metab. 82 (1997) 3516–3517.
[11] D.D. Bikle, Endocr. Rev. 13 (1992) 765–784.
[12] J. Reichrath, A. Perez, S.M. Muller, T.C. Chen, A. Kerber, F.A. Bahmer, M.F. Holick, Acta. Derm. Venereol. 77 (1997) 268–272.
[13] J.R. Snyman, K. de Sommers, M.A. Steinmann, D.J. Lizamore, Eur. J. Clin. Pharmacol. 52 (1997) 277–280.
[14] M. Shiraki, H. Orimo, H. Ito, I. Akiguchi, J. Nakao, R. Takahashi, S. Ishizuka, Endocrinol. Jpn. 32 (1985) 305–315.
[15] R. Bouillon, W.H. Okamura, A.W. Norman, Endocr. Rev. 16 (1995) 200–257.
[16] J. Abe, M. Morikawa, K. Miyamoto, S. Kaiho, M. Fukushima, C. Miyaura, E. Abe, T. Suda, Y. Nishii, FEBS Lett. 226 (1987) 58–62.
[17] J. Abe, T. Nakano, Y. Nishii, T. Matsumoto, E. Ogata, K. Ikeda, Endocrinology 129 (1991) 832–837.
[18] G. Jones, S.A. Strugnell, H.F. DeLuca, Physiol. Rev. 78 (1998) 1193–1231.
[19] H.M. Maung, L. Elangovan, J.M. Frazao, J.D. Bower, B.J. Kelley, S.R. Acchiardo, H.J. Rodriguez, K.C. Norris, J.F. Sigala, M. Rutkowski, J.A. Robertson, W.G. Goodman, B.S. Levine, R.W. Chesney, R.B. Mazess, D.M. Kyllo, L.L. Douglass, C.W. Bishop, J.W. Coburn, Am. J. Kidney Dis. 37 (2001) 532–543.
[20] S. Morimoto, S. Imanaka, E. Koh, T. Shiraishi, T. Nabata, S. Kitano, Y. Miyashita, Y. Nishii, T. Ogihara, Biochem. Int. 19 (1989) 1143–1149.
[21] B. Stabert, J. Roed-Petersen, T. Menne, Acta Derm. Venereol. (Stockh.) 69 (1989) 147–150.
[22] M.J. Calverley, Tetrahedron 43 (1987) 4609–4619.
[23] A.M. Thayer, Chem. Eng. News June 5 (2006) 15–32.
[24] V.A. Soloshonok, K. Mikami, T. Yamazaki, J.T. Welch, J. Honek (Eds.), Current Fluoroorganic Chemistry: New Synthetic Directions, Technologies, Materials, and Biological Applications, American Chemical Society, Washington, DC, 2006.
[25] J.A. Ma, D. Cahard, Chem. Rev. 104 (2004) 6119–6146.
[26] K. Mikami, Y. Itoh, M. Yamanaka, Chem. Rev. 104 (2004) 1–16.
[27] T. Hiyama, K. Kanie, T. Kusumoto, Y. Morizawa, M. Shimizu, Organofluorine Compounds, Springer, Berlin, 2000.
[28] R.E. Banks, B.E. Smart, J.C. Tatlow (Eds.), Organofluorine Chemistry: Principles and Commercial Applications, Plenum Press, New York, 1994.
[29] I. Ojima, J.R. McCarthy, J.T. Welch (Eds.), Biomedical Frontiers of Fluorine Chemistry, American Chemical Society, Washington, DC, 1996.
[30] J. Oshida, M. Morisaki, N. Ikekawa, Tetrahedr. Lett. 21 (1980) 1755–1756.
[31] E. Ohshima, S. Takatsuto, N. Ikekawa, H.F. DeLuca, Chem. Pharm. Bull. 32 (1984) 3518–3524.
[32] K. Mikami, S. Ohba, H. Ohmura, J. Organomet. Chem. 662 (2002) 77–82.
[33] Y. Itoh, S. Jang, S. Ohba, K. Mikami, Chem. Lett. 33 (2004) 776–777.
[34] K. Mikami, M. Yamanaka, M. Hatano, K. Aikawa, Org. React., in press.
[35] K. Mikami, K.M. Shimizu, Chem. Rev. 92 (1992) 1021–1050.
[36] B. Lythgoe, Chem. Soc. Rev. 9 (1980) 449–473.
[37] B. Lythgoe, T.A. Moran, M.E.N. Nambudiry, S. Ruston, J. Chem. Soc., Perkin I (1976) 2386–2390.
[38] K. Mikami, S. Ohba, H. Ohmura, N. Kubodera, K. Nakagawa, T. Okano, Chirality 13 (2001) 366–371.
[39] K. Mikami, A. Osawa, E. Isaka, M. Sawa, M. Shimizu, M. Terada, N. Kubodera, K. Nakagawa, N. Tsugawa, T. Okano, Tetrahedr. Lett. 39 (2001) 3359–3362.
[40] T. Kobayashi, N. Tsugawa, T. Okano, S. Masuda, A. Takeuchi, N. Kubodera, Y. Nishii, J. Biochem. 115 (1994) 373–380.
[41] K. Nakagawa, Y. Sasaki, S. Kato, N. Kubodera, T. Okano, Carcinogenesis 26 (2005) 1044–1054.
[42] K. Takeyama, Y. Masuhiro, H. Fuse, H. Endoh, A. Murayama, S. Kitanaka, M. Suzawa, J. Yanagisawa, S. Kato, Mol. Cell Biol. 19 (1999) 1049–1055.
[43] H. Yamamoto, N.K. Shevde, A. Warrier, L.A. Plum, H.F. DeLuca, J.W. Pike, J. Biol. Chem. 278 (2003) 31756–31765.
[44] K. Nakagawa, A. Kawaura, S. Kato, E. Takeda, T. Okano, Carcinogenesis 26 (2005) 429–440.
[45] T. Yoshizawa, Y. Handa, Y. Uematsu, S. Takeda, K. Sekine, Y. Yoshihara, T. Kawakami, K. Arioka, H. Sato, Y. Uchiyama, S. Masushige, A. Fukamizu, T. Matsumoto, S. Kato, Nat. Genet. 6 (1997) 391–396.
[46] C.D. Reddy, R. Patti, A. Guttapalli, J.M. Maris, N. Yanamanadra, A. Rachamallu, L.N. Sutton, P.C. Phillips, G.H., J. Cell. Biochem. 97 (2006) 198–206.
[47] M.I. Mohamed, M.J. Beckman, J. Meehan, H.F. DeLuca, Biochem. Biophys. Acta 1289 (1996) 275–283.
[48] M.T. Cantorna, J. Humpal-Winter, H.F. DeLuca, J. Nutr. 129 (1999) 1966–1971.
[49] Y. Ohyama, K. Ozono, M. Uchida, M. Yoshimura, T. Shinki, T. Suda, O. Yamamoto, J. Biol. Chem. 271 (1996) 30381–30385.
[50] S.A. Onte, S.Y. Tsai, M.J. Tsai, B.W. O'Malley, Science 270 (1995) 1354–1357.